Research Square

Preprints are preliminary reports that have not undergone peer review.
They should not be considered conclusive, used to inform clinical practice,
or referenced by the media as validated information.

Geometry-Preserving Optimal Control of Implicitly Singularly Perturbed Systems with Sliding and Exit Constraints

Volodymyr Gotsulenko

gosul@ukr.net

Institute of Engineering Thermophysics

Research Article

Keywords: optimal control, implicitly singularly perturbed systems, state constraints, singular regularization, sliding dynamics, control barrier functions

Posted Date: September 18th, 2026

DOI: https://doi.org/10.21203/rs.3.rs-10909736/v1

License: This work is licensed under a Creative Commons Attribution 4.0 International License.
Read Full License

Additional Declarations: No competing interests reported.

Version of Record: A version of this preprint was published at International Journal of Dynamics and Control on October 20th, 2026. See the published version at https://doi.org/10.1007/s40435-026-02355-z.

Geometry-Preserving Optimal Control of Implicitly Singularly Perturbed Systems with Sliding and Exit Constraints

Abstract

We study optimal regulation for a class of implicitly singularly perturbed nonlinear systems, in which an ordinary control-affine state equation is coupled to a second equation whose state-dependent coefficient loses rank on a dynamically accessible hypersurface. Actuation enters only the ordinary equation, so the controller reshapes tangential motion without displacing the loss-of-rank set or its exit boundary. We introduce a reciprocal Cauchy regularization that, for every positive value of a regularization parameter, selects an exact invariant reduced dynamics on the singular hyperplane. On compact subsets of the attracting region, trajectories contract toward this hyperplane at a rate that grows as the inverse square of the regularization parameter, together with a matching bound showing that the tangential deviation from the reduced dynamics shrinks quadratically in the regularization parameter and in the initial offset from the singular set; the result extends to locally Lipschitz feedback. When the initial state, reference, and terminal target all lie on the singular hyperplane, the full regularized problem and the reduced, lower-dimensional problem coincide exactly – same trajectories, costs, optimal values, minimizers, tangential Pontryagin systems, and restricted value functions – for every value of the regularization parameter, and this equivalence persists under identical tangential path constraints. For an initial offset comparable in size to the regularization parameter, the two problems' costs stay uniformly close, with the gap shrinking cubically in that parameter; the same cubic closeness holds for the optimal values for starting times bounded away from the terminal time, under a common safety-core assumption. Exit avoidance is posed as a genuine state-constrained optimal-control problem, while barrier-function inequalities, including a high-order extension for constraints of higher relative degree, form a separate, real-time safety layer rather than being folded into the transcription. A nonlinear Lyapunov argument built on a linear-quadratic Riccati baseline certifies an invariant safe ellipsoid for the Duffing–Rayleigh example. The same example's constrained direct-transcription solution is cross-checked by two independent nonlinear optimization solvers, and full simulations of the regularized system confirm rapid collapse onto the selected reduced dynamics.

Keywords: optimal control, implicitly singularly perturbed systems, state constraints, singular regularization, sliding dynamics, control barrier functions

1 Introduction

Implicit differential systems in which a state-dependent coefficient loses rank or vanishes can exhibit impasse sets, state-generated time-scale separation, sliding-like motion, and rapid excursions. Such phenomena occur in constrained differential equations and in implicitly singularly perturbed models of mechanical, fluid, thermal, and turbomachinery dynamics [1–4]. A representative uncontrolled model is

$$\begin{cases} \dot{\boldsymbol{x}} = \boldsymbol{f}(\boldsymbol{x}, y), \\ \varphi(y)\dot{y} = g(\boldsymbol{x}, y), \end{cases} \boldsymbol{x} \in \mathbb{R}^{n-1},\ y \in \mathbb{R}. \tag{1}$$

where $\varphi(y^*) = 0$ and $\varphi'(y^*) \neq 0$. The reciprocal field g/φ is unbounded at $y = y^*$, so the singular geometry is related to, but is not identical with, the classical setting of a locally essentially bounded Filippov vector field [5–7].

Several neighboring theories are relevant. Constrained differential systems with impasse singularities have been analyzed geometrically and related to singular perturbations [1, 2]. Classical singular-perturbation control, by contrast, starts from an explicit small-parameter slow–fast model and develops reduced and boundary-layer control problems [8]. Optimal control of differential-algebraic equations (DAEs) provides existence, necessary conditions, index-reduction techniques, and numerical methods for regular linear and nonlinear descriptor systems [9–12]. In particular, regular linear DAEs can be transformed to augmented ordinary differential equation (ODE) formulations under suitable input-index and consistency assumptions [12], while nonlinear DAEs of finite or arbitrary index admit dedicated maximum-principle formulations [10, 11]. A separate line of work derives necessary optimality conditions directly for *implicit* control systems in which the constraint Jacobian may be genuinely singular, using constraint-qualification or calmness conditions in place of a fixed DAE index [13–15]. That theory is posed abstractly, along a general admissible trajectory, and does not track a specific state-dependent loss-of-rank hypersurface, its exit boundary, or an explicit regularization family; the present paper instead exploits the concrete geometry of a scalar coefficient vanishing on a hypersurface to obtain an exact finite-dimensional on-manifold reduction together with quantitative off-manifold estimates. Piecewise-smooth optimal-control problems have also been approached through smooth singular-perturbation regularizations [16], and genuinely discontinuous systems containing sliding arcs require nonsmooth optimality machinery [17]. The comparison with Westenbroek et al. is especially useful: their singular-perturbation construction smooths general piecewise-smooth control systems and establishes consistency in the vanishing-perturbation limit, whereas the present reciprocal construction is tied to a specified state-dependent rank-loss factor and enforces $R_\epsilon(y^*) = 0$. Consequently, the hypersurface S is exactly invariant for every fixed $\epsilon > 0$, and the on-manifold state map and optimal-control problem coincide exactly rather than only asymptotically as $\epsilon \to 0$. The two approaches are therefore complementary: the former retains greater nonsmooth-system generality, while the latter sacrifices that generality in order to preserve a prescribed singular geometry exactly. Finally, pathwise state constraints lead to measure or bounded-variation multipliers and boundary-arc conditions rather than to the unconstrained Pontryagin equations alone [18–20].

The present problem is not a regular fixed-index DAE posed on a preassigned consistency manifold. It can be written as $E(\boldsymbol{z})\dot{\boldsymbol{z}} = F(\boldsymbol{z}, \boldsymbol{u})$ with

$$E(\boldsymbol{z}) = \begin{bmatrix} I_{n-1} & 0 \\ 0 & \varphi(y) \end{bmatrix},$$

whose rank drops on the state-dependent hypersurface $S = \{y = y^*\}$. This hypersurface is dynamically approached, and its attracting region, exit boundary, and accessibility are themselves part of the control problem. Thus the key issue is control relative to a loss-of-rank set, not merely consistency on a regular descriptor manifold. The reciprocal regularization used below is designed to preserve that hypersurface exactly and to select a generalized lower-dimensional dynamics on it.

We consider *regular-channel actuation*, $\dot{\boldsymbol{x}} = \boldsymbol{f}(\boldsymbol{x}, y) + \boldsymbol{B}(\boldsymbol{x}, y)\boldsymbol{u}$, $\varphi(y)\dot{y} = g(\boldsymbol{x}, y)$, so that the controller changes tangential motion without moving the singular hyperplane or the associated exit set. This restriction is essential: direct control in the singular equation would define a different problem because it could create, cancel, or displace the singular transition.

The paper is organized around the loss-of-rank geometry and the optimal-control consequences of a dedicated regularization. Existing theories address regular DAE optimal control, nonsmooth optimal control with sliding modes, and regularization of piecewise-smooth vector fields. The class considered here differs because a state-dependent coefficient vanishes on a dynamically accessible loss-of-rank hypersurface. The control objective is therefore coupled to attraction toward, and exit from, this singular set. The proposed reciprocal regularization preserves the hypersurface exactly, selects a lower-dimensional generalized dynamics on it, and permits both exact on-manifold optimal-control reduction and quantitative off-manifold consistency estimates.

The main contributions are as follows:

- a regular-channel control architecture that modifies tangential motion without moving the state-dependent loss-of-rank hypersurface or its exit set;
- a reciprocal Cauchy regularization that selects an exact invariant generalized dynamics on S for every $\epsilon > 0$, together with uniform normal attraction and a nonlinear normal-tube contraction estimate;
- the quantitative tangential estimate $\|\boldsymbol{x}_\epsilon(t) - \boldsymbol{x}_s(t)\| \le C_T\epsilon^2|y_\epsilon(0) - y^*|$ on fixed finite horizons, plus an extension to locally Lipschitz state feedback;
- an exact on-manifold optimal-control equivalence theorem: for every $\epsilon > 0$ the regularized and selected lower-dimensional problems have identical state maps, costs, optimal values, minimizers, tangential Pontryagin minimum principle (PMP) systems, and restricted value functions, with the same equivalence retained under tangential path constraints such as the exit margin;
- a uniform off-manifold consistency result for costs, together with an optimal-value estimate uniform on compact subintervals bounded away from the terminal time; both have $O(\epsilon^3)$ accuracy for $O(\epsilon)$ normal initial offsets under a common safety-core hypothesis;

- an exit-constrained optimal-control formulation, with boundary-arc geometry separated explicitly from real-time control barrier function (CBF) and high-order control barrier function (HOCBF) filtering;
- a computable nonlinear Lyapunov/Riccati certificate that is simultaneously invariant, actuator-compatible, and strictly separated from the singular exit;
- constrained nonlinear finite-horizon computations independently cross-checked by two nonlinear-programming solvers, together with full regularized simulations and additional analytical validation examples.

Classical existence results, the PMP, Hamilton–Jacobi–Bellman (HJB) theory, the continuous-time algebraic Riccati equation (CARE), linear-quadratic regulator (LQR) design, and CBF constructions are used only as tools. The claimed novelty lies in their interaction with the state-dependent loss-of-rank geometry, the regularization-selected dynamics, and the resulting exact and asymptotic optimal-control consistency properties.

2 Controlled implicitly singularly perturbed system

2.1 State equations and geometry

We consider

$$\begin{cases} \dot{\boldsymbol{x}} = \boldsymbol{f}(\boldsymbol{x}, y) + \boldsymbol{B}(\boldsymbol{x}, y)\boldsymbol{u}, \\ \varphi(y)\dot{y} = g(\boldsymbol{x}, y). \end{cases} \tag{2}$$

where $\boldsymbol{u}(t) \in U \subset \mathbb{R}^m$, U is compact and convex, $\boldsymbol{f}, g, \boldsymbol{B}$ are continuously differentiable, and $\varphi \in C^1$ has a simple zero $\varphi(y^*) = 0$, $\varphi'(y^*) \neq 0$. Define $S = \{(\boldsymbol{x}, y) : y = y^*\}$, $\Sigma = \{(\boldsymbol{x}, y^*) : g(\boldsymbol{x}, y^*) = 0\}$. We assume $\nabla_{\boldsymbol{x}} g \neq 0$ on Σ, so Σ is a smooth codimension-one submanifold of S. Let $a = -\operatorname{sgn}\varphi'(y^*)$, $h(\boldsymbol{x}) := a\, g(\boldsymbol{x}, y^*)$. The sliding domain and its closed safety core are

$$\mathcal{D} = \{\boldsymbol{x} : h(\boldsymbol{x}) > 0\},\ \mathcal{D}_\delta = \{\boldsymbol{x} : h(\boldsymbol{x}) \geq \delta\},\ \delta > 0. \tag{3}$$

Thus Σ is the zero level of the exit function h. The sign convention is chosen so that positive h corresponds to attracting sliding.

Remark 2.1. The restriction of the actuator to the $\boldsymbol{x}$-equation is structural rather than cosmetic. If the singular equation were changed to $\varphi(y)\dot{y} = g(\boldsymbol{x}, y) + c(\boldsymbol{x}, y)^T\boldsymbol{u}$, the controller would move the exit manifold and could cancel or create the singular transition. Regular-channel actuation instead changes the tangential motion while leaving S, Σ, and the sign condition (3) intact.

2.2 Sliding geometry and the role of regularization

For $y = y^* \pm \eta$ with $\eta > 0$ small, the normal component of the formal vector field is g/φ. On $\mathcal{D}$ these one-sided normal velocities have opposite signs and their magnitudes diverge as $\eta \downarrow 0$. This is the geometric signature of an attracting sliding configuration. However, because g/φ is unbounded at S, we do not invoke the classical Filippov set-valued construction as the definition of a solution on the singular hyperplane.

Instead, the sliding dynamics used throughout this paper is selected by the geometry-preserving reciprocal regularization introduced in the next section. The key

point is stronger than a formal convex-combination argument: the regularized system leaves S exactly invariant for every $\epsilon > 0$, and its restriction to S is independent of ϵ. Thus the lower-dimensional control system on the singular hyperplane is obtained as an exact invariant subsystem rather than as an ambiguous evaluation of an unbounded vector field.

Remark 2.2 (Relation with Filippov sliding). The opposite signs of the divergent normal velocities provide the same attracting/repelling geometric classification that motivates sliding in Filippov systems. We therefore retain the term *sliding domain* for $\mathcal{D}$. The mathematical selection used here, however, is the exact invariant regularization below; no claim is made that the unbounded field g/φ itself satisfies the standard hypotheses of classical Filippov solution theory.

Remark 2.3 (Classical impasse versus selected dynamics). Inside $\mathcal{D}$, one has $g(\boldsymbol{x}, y^*) \neq 0$. Therefore substituting $y = y^*$ into the original implicit equation would give the inconsistent algebraic relation $0 = g(\boldsymbol{x}, y^*)$. Consequently, $(\boldsymbol{x}(t), y^*)$ is not claimed to be a classical solution of the original implicit system in the sliding domain. The on-manifold dynamics introduced below is instead a generalized dynamics selected by the reciprocal regularization. This distinction is essential when comparing the present construction with regular DAE optimal control.

3 Exact Cauchy regularization and finite-horizon optimal control

Direct optimization of (2) is inconvenient because g/φ is unbounded. For $\epsilon > 0$, define the Cauchy-type reciprocal regularization

$$R_\epsilon(y) = \frac{\varphi(y)}{\varphi(y)^2 + \epsilon^2}. \tag{4}$$

Then $R_\epsilon \in C^1$, $R_\epsilon(y^*) = 0$, and $R_\epsilon(y) \longrightarrow \frac{1}{\varphi(y)}$ locally uniformly on compact subsets not intersecting $\{\varphi = 0\}$. The regularized controlled dynamics is

$$\begin{cases} \dot{\boldsymbol{x}} = \boldsymbol{f}(\boldsymbol{x}, y) + \boldsymbol{B}(\boldsymbol{x}, y)\boldsymbol{u}, \\ \dot{y} = g(\boldsymbol{x}, y) R_\epsilon(y). \end{cases} \tag{5}$$

Theorem 3.1 (Exact invariance and normal attraction)**.** *For every $\epsilon > 0$ and every admissible control, the hyperplane $S = \{y = y^*\}$ is invariant under* (5)*. Along S, the normal linearization is*

$$\lambda_\perp(\boldsymbol{x}, \epsilon) = \frac{\partial}{\partial y}\big[g(\boldsymbol{x}, y) R_\epsilon(y)\big]\Big|_{y=y^*} = -\frac{|\varphi'(y^*)|}{\epsilon^2}\, h(\boldsymbol{x}). \tag{6}$$

Consequently, on every compact $K \subset \mathcal{D}_\delta$, $\lambda_\perp(\boldsymbol{x}, \epsilon) \leq -\frac{|\varphi'(y^*)|\delta}{\epsilon^2} < 0$, $\boldsymbol{x} \in K$, so S is uniformly normally attracting over K with linear attraction rate of order ϵ^{-2}.

Proof For fixed $\epsilon > 0$, the denominator in (4) is strictly positive. Since φ, g, $\boldsymbol{f}$, and $\boldsymbol{B}$ are continuously differentiable, the regularized vector field is locally Lipschitz in the state. Hence

the regularized initial-value problem has a unique local solution for every locally bounded admissible control.

At $y = y^*$, one has $\varphi(y^*) = 0$, and therefore $R_\epsilon(y^*) = \frac{\varphi(y^*)}{\varphi(y^*)^2+\epsilon^2} = 0$. Thus the normal component of the regularized vector field vanishes identically on S: $\dot{y} = g(\boldsymbol{x}, y^*)R_\epsilon(y^*) = 0$. Consequently the vector field is tangent to S, and uniqueness implies invariance of S.

To compute the normal linearization, differentiate the normal right-hand side: $\partial_y(gR_\epsilon) = g_y R_\epsilon + gR'_\epsilon$. For $R_\epsilon(y) = \frac{\varphi(y)}{\varphi(y)^2+\epsilon^2}$, direct differentiation gives

$$R'_\epsilon(y) = \frac{\varphi'(y)\big(\epsilon^2 - \varphi(y)^2\big)}{\big(\varphi(y)^2 + \epsilon^2\big)^2}.$$

At $y = y^*$, this reduces to $R'_\epsilon(y^*) = \frac{\varphi'(y^*)}{\epsilon^2}$. Because $R_\epsilon(y^*) = 0$, the first term $g_y R_\epsilon$ disappears and $\lambda_\perp(\boldsymbol{x}, \epsilon) = g(\boldsymbol{x}, y^*)\frac{\varphi'(y^*)}{\epsilon^2}$. By definition, $h(\boldsymbol{x}) = -\operatorname{sgn}(\varphi'(y^*))g(\boldsymbol{x}, y^*)$, so $g(\boldsymbol{x}, y^*)\varphi'(y^*) = -|\varphi'(y^*)|h(\boldsymbol{x})$, which proves (6). If $\boldsymbol{x} \in K \subset \mathcal{D}_\delta$, then $h(\boldsymbol{x}) \geq \delta$, hence $\lambda_\perp(\boldsymbol{x}, \epsilon) \leq -\frac{|\varphi'(y^*)|\delta}{\epsilon^2}$. This estimate is uniform in $\boldsymbol{x} \in K$, and the asserted linear normal-attraction rate follows. □

Theorem 3.2 (Normal-tube contraction and tangential convergence)**.** *Let $K_0 \Subset K \Subset \mathcal{D}_\delta$ be compact sets. Fix $T > 0$ and an admissible control $\boldsymbol{u}(\cdot)$. Assume that the selected on-manifold solution $\boldsymbol{x}_s(t)$ of (10), with $\boldsymbol{x}_s(0) = \boldsymbol{x}_0 \in K_0$, remains in K_0 on $[0, T]$. Then there exist constants $c > 0$, $C_T > 0$, $r > 0$, and $\epsilon_0 > 0$, independent of ϵ, such that for every $0 < \epsilon \leq \epsilon_0$ and every regularized initial condition $\boldsymbol{x}_\epsilon(0) = \boldsymbol{x}_0$, $|y_\epsilon(0) - y^*| \leq r\epsilon$, the regularized solution exists on $[0, T]$, remains in $K \times \{|y - y^*| \leq r\epsilon\}$, and satisfies*

$$|y_\epsilon(t) - y^*| \leq |y_\epsilon(0) - y^*| \exp\left(-\frac{ct}{\epsilon^2}\right),\ 0 \leq t \leq T. \tag{7}$$

and

$$\|\boldsymbol{x}_\epsilon(t) - \boldsymbol{x}_s(t)\| \leq C_T\epsilon^2|y_\epsilon(0) - y^*|,\ 0 \leq t \leq T. \tag{8}$$

The constants can be selected quantitatively from compact-set data. In particular, put $m_0 := |\varphi'(y^*)|\delta$, choose $e_0 > 0$ so that

$$\sup_{\substack{\boldsymbol{x}\in K\\ |e|\leq e_0}} |q(\boldsymbol{x}, e) - q(\boldsymbol{x}, 0)| \leq \frac{m_0}{2},\ q(\boldsymbol{x}, e) := g(\boldsymbol{x}, y^* + e)\frac{\varphi(y^* + e)}{e}.$$

with the quotient continuously extended at $e = 0$, and define $M_\varphi := \sup_{|e|\leq e_0} |\varphi'(y^* + e)|$, $c_0 := \frac{m_0}{2}$. For any fixed $r > 0$, define the compact-tube derivative bounds

$$L_x := \sup_{K\times[y^*-e_0, y^*+e_0]\times U} \|D_{\boldsymbol{x}} F_x\|,\ L_y := \sup_{K\times[y^*-e_0, y^*+e_0]\times U} \|\partial_y F_x\|.$$

where $F_x = \boldsymbol{f} + \boldsymbol{B}\boldsymbol{u}$ and the matrix norm is the induced Euclidean norm, and set $c = \frac{c_0}{1+M_\varphi^2 r^2}$, $C_T = \frac{L_y}{c}e^{L_x T}$. Finally let $d_K := \operatorname{dist}(K_0, \mathbb{R}^{n-1} \setminus \operatorname{int} K) > 0$ and choose, for example,

$$0 < \epsilon_0 < \min\left\{\frac{e_0}{r}, \left(\frac{d_K}{C_T r}\right)^{1/3}\right\}.$$

Thus c, C_T, e_0, and an admissible ϵ_0 are all determined by the indicated compact tube, the safety margin δ, r, and the fixed horizon T, not by the running value of ϵ. In particular, if the initial normal displacement is $O(\epsilon)$, then the generic tangential deviation is $O(\epsilon^3)$ on a fixed finite interval.

Proof Put $e = y - y^*$. For $e \neq 0$, define $q(\boldsymbol{x}, e) := g(\boldsymbol{x}, y^* + e)\frac{\varphi(y^*+e)}{e}$. Because $\varphi \in C^1$ and $\varphi(y^*) = 0$, the quotient $\varphi(y^* + e)/e$ extends continuously to $e = 0$ with value $\varphi'(y^*)$. Hence q extends continuously to $q(\boldsymbol{x}, 0) = g(\boldsymbol{x}, y^*)\varphi'(y^*) = -|\varphi'(y^*)|h(\boldsymbol{x})$. Since $K \subset \mathcal{D}_\delta$, $q(\boldsymbol{x}, 0) \leq -|\varphi'(y^*)|\delta =: -m_0 < 0$ ($\boldsymbol{x} \in K$). To make this bound uniform for small $e \neq 0$, fix any $\bar{e} > 0$. Because $\varphi \in C^1$, writing $\varphi(y^* + e) = \int_0^1 \varphi'(y^* + \tau e)\, e\, d\tau$ shows that $(\boldsymbol{x}, e) \mapsto \varphi(y^*+e)/e := \int_0^1 \varphi'(y^*+\tau e)\, d\tau$ is continuous on $\mathbb{R}\times[-\bar{e}, \bar{e}]$, including at $e = 0$, where it equals $\varphi'(y^*)$; since $g \in C^1$, the product $q(\boldsymbol{x}, e) = g(\boldsymbol{x}, y^* + e) \cdot \big(\varphi(y^* + e)/e\big)$ is therefore continuous on the compact set $K \times [-\bar{e}, \bar{e}]$, hence uniformly continuous there. Uniform continuity supplies $e_0 \in (0, \bar{e}]$ such that $|q(\boldsymbol{x}, e) - q(\boldsymbol{x}, 0)| < \frac{m_0}{2}$ whenever $\boldsymbol{x} \in K,\ |e| \leq e_0$, and combining this with $q(\boldsymbol{x}, 0) \leq -m_0$ gives

$$q(\boldsymbol{x}, e) \leq -c_0 < 0,\ \boldsymbol{x} \in K,\ |e| \leq e_0,\ c_0 := \frac{m_0}{2}. \tag{9}$$

Because $\varphi \in C^1$, the compact interval $[y^* - e_0, y^* + e_0]$ gives the explicit derivative bound $M_\varphi := \sup_{|e|\leq e_0} |\varphi'(y^* + e)| < \infty$. The mean-value theorem therefore yields $|\varphi(y^* + e)| \leq M_\varphi|e|$ ($|e| \leq e_0$). Choose $r > 0$ and then $\epsilon_0 > 0$ so that $r\epsilon_0 \leq e_0$. As long as $|e(t)| \leq r\epsilon$ and $\boldsymbol{x}_\epsilon(t) \in K$, $\varphi(y^* + e)^2 + \epsilon^2 \leq (M_\varphi^2 r^2 + 1)\epsilon^2$. Using $\dot{e} = \dot{y}$ and the definition of q,

$$\frac{1}{2}\frac{d}{dt}e^2 = e\, g(\boldsymbol{x}, y^* + e)\frac{\varphi(y^* + e)}{\varphi(y^* + e)^2 + \epsilon^2} = \frac{q(\boldsymbol{x}, e)}{\varphi(y^* + e)^2 + \epsilon^2}e^2.$$

Together with (9), this yields $\frac{1}{2}\frac{d}{dt}e^2 \leq -\frac{c_0}{(1+M_\varphi^2 r^2)\epsilon^2}e^2$. Set $c := \frac{c_0}{1+M_\varphi^2 r^2} > 0$. Gronwall's inequality gives (7). In particular, $|e(t)|$ is nonincreasing, so the normal tube $|e| \leq r\epsilon$ is positively invariant as long as the tangential component remains in K.

We next estimate the tangential error. Let $F_x(\boldsymbol{x}, y, \boldsymbol{u}) := \boldsymbol{f}(\boldsymbol{x}, y) + \boldsymbol{B}(\boldsymbol{x}, y)\boldsymbol{u}$. Since U is compact and F_x is continuously differentiable, the compact tube $K \times [y^* - e_0, y^* + e_0] \times U$ admits finite constants $L_x, L_y > 0$, for example any bounds satisfying $\|F_x(\boldsymbol{x}_1, y_1, \boldsymbol{u}) - F_x(\boldsymbol{x}_2, y_2, \boldsymbol{u})\| \leq L_x\|\boldsymbol{x}_1 - \boldsymbol{x}_2\| + L_y|y_1 - y_2|$. With $d(t) = \|\boldsymbol{x}_\epsilon(t) - \boldsymbol{x}_s(t)\|$ and identical initial tangential states, $d(t) \leq L_x \int_0^t d(s)\, ds + L_y \int_0^t |e(s)|\, ds$. Using (7), $\int_0^t |e(s)|\, ds \leq |e(0)| \int_0^t e^{-cs/\epsilon^2}\, ds \leq \frac{\epsilon^2}{c}|e(0)|$. A second application of Gronwall's inequality gives $d(t) \leq \frac{L_y}{c}e^{L_x T}\epsilon^2|e(0)|$, so (8) holds with $C_T = \frac{L_y}{c}e^{L_x T}$. Finally, because $K_0 \Subset K$, the distance from K_0 to ∂K is positive. By choosing ϵ_0 smaller if needed, the right-hand side of (8) is strictly less than this distance. A standard continuation argument then prevents $\boldsymbol{x}_\epsilon$ from reaching ∂K before time T. Thus the bootstrap assumptions used above hold on all of $[0, T]$, completing the proof. □

Corollary 3.3 (Normal-tube contraction under locally Lipschitz feedback)**.** *Assume the hypotheses of Theorem 3.2 and let $\boldsymbol{u} = k(\boldsymbol{x})$, where k is locally Lipschitz on a neighborhood of K and $k(K) \subset U$. Let $\boldsymbol{x}_s$ solve the selected closed-loop dynamics $\dot{\boldsymbol{x}}_s = \boldsymbol{f}(\boldsymbol{x}_s, y^*) + \boldsymbol{B}(\boldsymbol{x}_s, y^*)k(\boldsymbol{x}_s)$ and assume $\boldsymbol{x}_s([0, T]) \subset K_0$. Then, after possibly reducing ϵ_0, the estimates* (7) *and* (8) *remain valid for the full regularized feedback system. In particular,*

$$|y_\epsilon(t) - y^*| \leq |e_0|e^{-ct/\epsilon^2},\ \|\boldsymbol{x}_\epsilon(t) - \boldsymbol{x}_s(t)\| \leq C_T^{\mathrm{fb}}\epsilon^2|e_0|.$$

Proof Define the closed-loop tangential field $F_{\mathrm{cl}}(\boldsymbol{x}, y) = \boldsymbol{f}(\boldsymbol{x}, y) + \boldsymbol{B}(\boldsymbol{x}, y)k(\boldsymbol{x})$. Because $\boldsymbol{f}$ and $\boldsymbol{B}$ are C^1 and k is locally Lipschitz, F_{cl} is locally Lipschitz on a compact neighborhood of $K \times \{y^*\}$. Hence there are constants $\widetilde{L}_x, \widetilde{L}_y > 0$ such that

$$\|F_{\mathrm{cl}}(\boldsymbol{x}_1, y_1) - F_{\mathrm{cl}}(\boldsymbol{x}_2, y_2)\| \le \widetilde{L}_x \|\boldsymbol{x}_1 - \boldsymbol{x}_2\| + \widetilde{L}_y |y_1 - y_2|.$$

The normal equation is unchanged by the feedback because control acts only through the regular channel. Therefore the proof of Theorem 3.2 gives the same exponential normal estimate. Replacing L_x, L_y by $\widetilde{L}_x, \widetilde{L}_y$ in the tangential Gronwall estimate yields $\|\boldsymbol{x}_\epsilon(t) - \boldsymbol{x}_s(t)\| \le \frac{\widetilde{L}_y}{c} e^{\widetilde{L}_x T} \epsilon^2 |e_0|$. The continuation argument is identical, proving the claim. □

Definition 3.4 (Regularization-selected generalized sliding dynamics)**.** For the reciprocal regularization (4), the *regularization-selected generalized sliding dynamics* on $S = \{y = y^*\}$ is the tangential control system obtained by restricting the regularized vector field to its exact invariant hyperplane: $\dot{\boldsymbol{x}} = \boldsymbol{f}(\boldsymbol{x}, y^*) + \boldsymbol{B}(\boldsymbol{x}, y^*)\boldsymbol{u}$. This terminology does not identify $(\boldsymbol{x}(t), y^*)$ with a classical solution of the original implicit equation inside the impasse region; it denotes the generalized dynamics selected by the geometry-preserving regularization.

Proposition 3.5 (Exact invariant selected dynamics)**.** *Let $\epsilon > 0$, let $\boldsymbol{u}(\cdot)$ be any admissible locally bounded control, and let the initial condition satisfy $(\boldsymbol{x}(0), y(0)) = (\boldsymbol{x}_0, y^*)$. Then the solution of (5) satisfies $y(t) \equiv y^*$ for every time for which the solution exists. Its tangential component is therefore governed exactly by the selected dynamics*

$$\dot{\boldsymbol{x}} = \boldsymbol{f}_s(\boldsymbol{x}) + \boldsymbol{B}_s(\boldsymbol{x})\boldsymbol{u}, \ \boldsymbol{f}_s(\boldsymbol{x}) := \boldsymbol{f}(\boldsymbol{x}, y^*), \ \boldsymbol{B}_s(\boldsymbol{x}) := \boldsymbol{B}(\boldsymbol{x}, y^*). \tag{10}$$

In particular, the selected on-manifold state dynamics is independent of ϵ.

Proof For fixed $\epsilon > 0$, Theorem 3.1 guarantees that the regularized vector field is locally Lipschitz and tangent to S. Consider the candidate normal component $\widehat{y}(t) \equiv y^*$. It satisfies the normal equation because $g(\boldsymbol{x}(t), y^*)R_\epsilon(y^*) = 0$ for every tangential trajectory $\boldsymbol{x}(t)$. Hence $(\boldsymbol{x}(t), \widehat{y}(t))$ solves the full regularized system precisely when $\boldsymbol{x}$ solves $\dot{\boldsymbol{x}} = \boldsymbol{f}(\boldsymbol{x}, y^*) + \boldsymbol{B}(\boldsymbol{x}, y^*)\boldsymbol{u}$. The regularized initial-value problem and this restricted initial-value problem have the same initial state $(\boldsymbol{x}_0, y^*)$. Uniqueness therefore excludes any second solution whose normal component leaves y^*. Thus $y(t) = y^*$ identically and the tangential equation is exactly (10). Since ϵ does not appear in (10), the selected invariant dynamics is independent of the regularization parameter. No singular limit and no Filippov convexification are involved. □

Corollary 3.6 (Parameter-independent invariant restriction of the regularized family)**.** *For every $\epsilon > 0$, restriction of the regularized state equation (5) to its exact invariant hyperplane S yields the same selected control system (10). Thus all members of the regularized family possess an identical on-manifold dynamics, independent of ϵ.*

Proof For every $\epsilon > 0$, $R_\epsilon(y^*) = 0$. Proposition 3.5 therefore gives $y(t) \equiv y^*$ and $\dot{\boldsymbol{x}} = \boldsymbol{f}(\boldsymbol{x}, y^*) + \boldsymbol{B}(\boldsymbol{x}, y^*)\boldsymbol{u}$. The right-hand side contains no occurrence of ϵ, so the invariant restriction of every regularized member is the same. No classical restriction of the original implicit equation is asserted; Remark 2.3 explains why such a restriction would be inconsistent inside $\mathcal{D}$. □

Proposition 3.7 (Minimal hypotheses for invariance versus normal attraction under a general regularizing family)**.** *Let $\{\widetilde{R}_\epsilon\}_{\epsilon>0} \subset C^1(\mathbb{R})$ be any family used in place of R_ϵ in* (5)*, with each $\widetilde{R}_\epsilon$ locally Lipschitz uniformly on compact sets, so that the corresponding initial-value problems are well posed. The following three properties require strictly increasing hypotheses on $\widetilde{R}_\epsilon$, and none of the later ones is implied by the earlier ones alone.*

(i) Invariance and selected dynamics. *If $\widetilde{R}_\epsilon(y^*) = 0$ for every $\epsilon > 0$, then S is exactly invariant under the resulting regularized field, and its restriction to S is exactly* (10)*, for every $\epsilon > 0$ and independently of the choice of $\widetilde{R}_\epsilon$. This is the entire content used in the proofs of Theorem 3.1's invariance claim and of Proposition 3.5: no hypothesis on $\widetilde{R}_\epsilon$ away from y^*, and none on $\widetilde{R}'_\epsilon(y^*)$, is needed for this part.*

(ii) Qualitative normal attraction needs an additional sign condition. *Suppose in addition that $\widetilde{R}_\epsilon$ is differentiable at y^*. Repeating the computation of Theorem 3.1 with R_ϵ replaced by $\widetilde{R}_\epsilon$ gives the normal linearization*

$$\widetilde{\lambda}_\perp(\boldsymbol{x}, \epsilon) = g(\boldsymbol{x}, y^*)\widetilde{R}'_\epsilon(y^*) = -\operatorname{sgn}\varphi'(y^*)\, h(\boldsymbol{x})\, \widetilde{R}'_\epsilon(y^*).$$

This is negative throughout the sliding domain $\mathcal{D} = \{h > 0\}$ – i.e., S is normally attracting on $\mathcal{D}$ for the family $\widetilde{R}_\epsilon$, with the same sliding domain as for R_ϵ – if and only if

$$\operatorname{sgn}\widetilde{R}'_\epsilon(y^*) = \operatorname{sgn}\varphi'(y^*) \text{ for every } \epsilon > 0. \tag{11}$$

Condition (11) *is emphatically not implied by $\widetilde{R}_\epsilon(y^*) = 0$: the constant choice $\widetilde{R}_\epsilon \equiv 0$ is locally Lipschitz and vanishes at y^*, satisfying (i) trivially, yet gives $\widetilde{\lambda}_\perp \equiv 0$ and no normal attraction whatsoever – indeed every hyperplane $\{y = \text{const}\}$, not only S, is then invariant, and the reduction, while still exact, is dynamically vacuous away from S. Invariance of S and normal attraction toward S are thus logically independent properties of the family, governed respectively by $\widetilde{R}_\epsilon(y^*) = 0$ and by* (11)*.*

(iii) The quantitative rate and the tube estimates are specific to the reciprocal family. *Even granting* (11)*, the particular rate $O(\epsilon^{-2})$ of Theorem 3.1 and the tube estimates of Theorem 3.2 use the exact scaling $R'_\epsilon(y^*) = \varphi'(y^*)/\epsilon^2$ together with the bound $\varphi(y)^2 + \epsilon^2 \le (1 + M_\varphi^2 r^2)\epsilon^2$ on the normal tube, both particular to the reciprocal form* (4)*. A family satisfying* (11) *with a different scaling of $\widetilde{R}'_\epsilon(y^*)$ in ϵ would still be normally attracting on $\mathcal{D}$, but with a different rate and different tube constants;* (11) *alone fixes only the sign, not the order, of the attraction.*

Proof Part (i) is Proposition 3.5 together with Corollary 3.6, whose proofs use only $\widetilde{R}_\epsilon(y^*) = 0$ and local Lipschitzness of $\widetilde{R}_\epsilon$, exactly as recorded there. For (ii), differentiating $g(\boldsymbol{x}, y)\widetilde{R}_\epsilon(y)$ at $y = y^*$ and using $\widetilde{R}_\epsilon(y^*) = 0$ exactly as in the proof of Theorem 3.1 gives $\widetilde{\lambda}_\perp(\boldsymbol{x}, \epsilon) = g(\boldsymbol{x}, y^*)\widetilde{R}'_\epsilon(y^*)$; substituting $g(\boldsymbol{x}, y^*) = -\operatorname{sgn}(\varphi'(y^*))h(\boldsymbol{x})$ yields the displayed formula, which is negative for every $\boldsymbol{x}$ with $h(\boldsymbol{x}) > 0$ precisely when $\operatorname{sgn}\varphi'(y^*)\,\widetilde{R}'_\epsilon(y^*) > 0$, i.e. (11); the degenerate case $\widetilde{R}_\epsilon \equiv 0$ is immediate by inspection. Part (iii) follows because the proof of Theorem 3.1 identifies the rate constant explicitly as $|\varphi'(y^*)|/\epsilon^2 = |R'_\epsilon(y^*)|$, and the proof of Theorem 3.2 controls the denominator $\varphi(y^* + e)^2 + \epsilon^2$ using the specific reciprocal form;

replacing $R'_\epsilon(y^*)$ by a differently ϵ-scaled quantity of the same sign reproduces the same qualitative argument with the corresponding rate and constants in place of ϵ^{-2} and C_T. □

Remark 3.8. Exact on-manifold reduction, part (i) above, is therefore a structural feature of any admissible family with $\widetilde{R}_\epsilon(y^*) = 0$, whereas normal attraction toward S – its occurrence, its sign, its rate, and the explicit tube constants used throughout Sections 8–9 – is a property of the specific reciprocal Cauchy family (4). This family satisfies (11) automatically, since $R'_\epsilon(y^*) = \varphi'(y^*)/\epsilon^2$ has the same sign as $\varphi'(y^*)$ for every $\epsilon > 0$, and it additionally satisfies $R_\epsilon(y) \to 1/\varphi(y)$ locally uniformly away from y^*, which is what licenses calling it a regularization of (2) rather than merely an invariance-preserving deformation. A family satisfying (i) alone, without (11), would still produce an exact but dynamically inert on-manifold reduction, with no normal attraction to justify treating S as a controlled sliding surface.

Writing $\boldsymbol{z} = (\boldsymbol{x}, y)$, define

$$F_\epsilon(\boldsymbol{z}, \boldsymbol{u}) = \begin{bmatrix} \boldsymbol{f}(\boldsymbol{x}, y) + \boldsymbol{B}(\boldsymbol{x}, y)\boldsymbol{u} \\ g(\boldsymbol{x}, y)R_\epsilon(y) \end{bmatrix}. \tag{12}$$

For a continuous reference $\boldsymbol{z}_r \in C([0,T];\mathbb{R}^n)$, terminal target $\boldsymbol{z}_T$, symmetric matrices $Q \succeq 0$, $Q_T \succeq 0$, and $R \succ 0$, consider

$$J_\epsilon(\boldsymbol{u}) = \frac{1}{2}(\boldsymbol{z}(T)-\boldsymbol{z}_T)^T Q_T(\boldsymbol{z}(T)-\boldsymbol{z}_T) + \frac{1}{2}\int_0^T (\boldsymbol{z}-\boldsymbol{z}_r)^T Q(\boldsymbol{z}-\boldsymbol{z}_r)\,dt + \frac{1}{2}\int_0^T \boldsymbol{u}^T R\boldsymbol{u}\,dt. \tag{13}$$

Theorem 3.9 (Existence for the regularized problem)**.** *Assume that U is nonempty, compact and convex; F_ϵ is locally Lipschitz in $\boldsymbol{z}$ uniformly in $\boldsymbol{u} \in U$; all admissible trajectories remain in a common compact set on $[0,T]$; and the running cost in* (13) *is convex in $\boldsymbol{u}$. Then, for every fixed $\epsilon > 0$, there exists an optimal measurable control $\boldsymbol{u}^*_\epsilon \in L^\infty([0,T], U)$.*

Proof Fix $\epsilon > 0$. Because F_ϵ is locally Lipschitz in the state uniformly with respect to $\boldsymbol{u} \in U$, every measurable essentially bounded control generates a unique absolutely continuous trajectory until it leaves a compact set. By hypothesis all admissible trajectories remain in one common compact set, so solutions exist on the whole interval $[0,T]$.

Let $\{\boldsymbol{u}_k\}$ be a minimizing sequence. Since U is compact, the controls are uniformly essentially bounded. The state derivatives $F_\epsilon(\boldsymbol{z}_k, \boldsymbol{u}_k)$ are uniformly bounded on the common compact state set times U. Therefore $\{\boldsymbol{z}_k\}$ is uniformly bounded and equi-Lipschitz. Arzelà–Ascoli gives a subsequence, not relabeled, with $\boldsymbol{z}_k \to \bar{\boldsymbol{z}}$ uniformly on $[0,T]$.

For each fixed state $\boldsymbol{z}$, the dynamics is affine in $\boldsymbol{u}$, while the running cost $\ell(t, \boldsymbol{z}, \boldsymbol{u}) = \frac{1}{2}(\boldsymbol{z}-\boldsymbol{z}_r)^T Q(\boldsymbol{z}-\boldsymbol{z}_r) + \frac{1}{2}\boldsymbol{u}^T R\boldsymbol{u}$ is convex in $\boldsymbol{u}$. Hence the Cesari velocity–epigraph set

$$\mathcal{V}(t, \boldsymbol{z}) = \{(F_\epsilon(\boldsymbol{z}, \boldsymbol{u}), \ell(t, \boldsymbol{z}, \boldsymbol{u}) + r) : \boldsymbol{u} \in U,\ r \geq 0\}$$

is convex and closed. The standard Filippov–Cesari existence theorem therefore gives an ordinary measurable control $\bar{\boldsymbol{u}}(t) \in U$, rather than merely a relaxed control, whose trajectory is $\bar{\boldsymbol{z}}$ and whose integral cost is no larger than the lower limit of the minimizing sequence. The terminal cost is continuous in $\boldsymbol{z}(T)$, so uniform convergence of the trajectories also passes the terminal term to the limit. Consequently $J_\epsilon(\bar{\boldsymbol{u}}) \leq \liminf_{k\to\infty} J_\epsilon(\boldsymbol{u}_k) = \inf_{\boldsymbol{u}} J_\epsilon(\boldsymbol{u})$. Thus $\bar{\boldsymbol{u}}$ is optimal. Since $\bar{\boldsymbol{u}}(t) \in U$ almost everywhere and U is compact, $\bar{\boldsymbol{u}} \in L^\infty([0,T], U)$. □

Remark 3.10 (A checkable sufficient condition for the compactness hypothesis). The a priori compactness hypothesis in Theorem 3.9 is guaranteed, for instance, by a one-sided linear growth bound: if there is a constant $C_0 > 0$ such that $\boldsymbol{z}^T F_\epsilon(\boldsymbol{z}, \boldsymbol{u}) \le C_0(1 + \|\boldsymbol{z}\|^2)$, $\boldsymbol{z} \in \mathbb{R}^n$, $\boldsymbol{u} \in U$. then along any solution of (5) on its interval of existence, $\frac{d}{dt}\|\boldsymbol{z}(t)\|^2 = 2\boldsymbol{z}(t)^T F_\epsilon(\boldsymbol{z}(t), \boldsymbol{u}(t)) \le 2C_0\big(1 + \|\boldsymbol{z}(t)\|^2\big)$. and integrating this linear differential inequality gives, for every t in the interval of existence, $\|\boldsymbol{z}(t)\|^2 \le (\|\boldsymbol{z}(0)\|^2 + 1)e^{2C_0 t} - 1 \le (\|\boldsymbol{z}(0)\|^2 + 1)e^{2C_0 T} - 1$. Hence no admissible trajectory issued from a given $\boldsymbol{z}(0)$ can escape the fixed compact ball of this radius before time T; in particular solutions exist on all of $[0, T]$ and, for fixed $\boldsymbol{z}(0)$, all admissible trajectories remain in one common compact set, as required by Theorem 3.9. This growth bound holds whenever $\boldsymbol{f}$, $\boldsymbol{B}$, and gR_ϵ are (locally, hence on the relevant sublevel sets, globally) Lipschitz with at most linear growth, and more generally whenever the nonlinear terms are dissipative at infinity. Where it fails globally, the same estimate applied on a known invariant or attracting neighborhood – such as the certified ellipsoid of Proposition 8.1 in the worked example of Section 8 – serves the same purpose locally, without requiring global dissipativity of the vector field.

4 Pontryagin minimum principle

Let $\lambda = (\boldsymbol{p}, \eta) \in \mathbb{R}^{n-1} \times \mathbb{R}$ be the costate. The necessary conditions below follow the classical Pontryagin formalism [21], in the formulations given in [22–25]. With the minimization convention, define

$$\begin{aligned} H_\epsilon(\boldsymbol{z}, \lambda, \boldsymbol{u}, t) = \frac{1}{2}(\boldsymbol{z} - \boldsymbol{z}_r)^T Q(\boldsymbol{z} - \boldsymbol{z}_r) + \frac{1}{2}\boldsymbol{u}^T R\boldsymbol{u} \\ + \boldsymbol{p}^T\big(\boldsymbol{f}(\boldsymbol{x}, y) + \boldsymbol{B}(\boldsymbol{x}, y)\boldsymbol{u}\big) + \eta g(\boldsymbol{x}, y) R_\epsilon(y). \end{aligned} \tag{14}$$

Theorem 4.1 (Necessary optimality conditions)**.** *Let $\boldsymbol{u}_\epsilon^*$ be an optimal control for (5)–(13). Under the stated differentiability assumptions, the extremal is normal. Hence the scalar PMP multiplier can be normalized to $\lambda_0 = 1$, and there exists an absolutely continuous costate $\lambda = (\boldsymbol{p}, \eta)$ such that*

$$\dot{\boldsymbol{z}} = \partial_\lambda H_\epsilon,\ \dot{\lambda} = -\partial_{\boldsymbol{z}} H_\epsilon, \tag{15}$$

with terminal condition $\lambda(T) = Q_T(\boldsymbol{z}(T) - \boldsymbol{z}_T)$, and, for almost every t,

$$\boldsymbol{u}_\epsilon^*(t) \in \arg\min_{v \in U} H_\epsilon(\boldsymbol{z}(t), \lambda(t), v, t). \tag{16}$$

Proof The classical PMP applied to the smooth regularized problem yields multipliers $(\lambda_0, \lambda(\cdot))$, with $\lambda_0 \ge 0$, not simultaneously zero, and Hamiltonian $\mathcal{H}_\epsilon = \lambda_0 \ell(t, \boldsymbol{z}, \boldsymbol{u}) + \lambda^T F_\epsilon(\boldsymbol{z}, \boldsymbol{u})$. Because the terminal state is free and the endpoint contribution is the smooth terminal penalty $\Phi(\boldsymbol{z}(T)) = \frac{1}{2}(\boldsymbol{z}(T) - \boldsymbol{z}_T)^T Q_T(\boldsymbol{z}(T) - \boldsymbol{z}_T)$, transversality gives $\lambda(T) = \lambda_0 \nabla\Phi(\boldsymbol{z}(T)) = \lambda_0 Q_T(\boldsymbol{z}(T) - \boldsymbol{z}_T)$. Suppose that an abnormal multiplier $\lambda_0 = 0$ were possible. Then $\lambda(T) = 0$. With $\lambda_0 = 0$, the adjoint equation contains only terms linear and homogeneous in λ: $\dot{\lambda} = -D_{\boldsymbol{z}} F_\epsilon(\boldsymbol{z}, \boldsymbol{u})^T \lambda$. The unique solution of this terminal-value linear homogeneous equation with $\lambda(T) = 0$ is $\lambda \equiv 0$, contradicting the PMP nontriviality condition. Hence $\lambda_0 > 0$, and division of all multipliers by λ_0 permits the normalization $\lambda_0 = 1$.

Under this normalization $\mathcal{H}_\epsilon$ becomes precisely H_ϵ in (14). The standard PMP state equation, adjoint equation, transversality condition, and pointwise minimum condition therefore reduce to (15)–(16). □

$$\dot{\boldsymbol{p}} = -Q_{x\bullet}(\boldsymbol{z} - \boldsymbol{z}_r) - D_x \boldsymbol{f}(\boldsymbol{x}, y)^T \boldsymbol{p} - \sum_{j=1}^{m} u_j D_x B_j(\boldsymbol{x}, y)^T \boldsymbol{p} - \eta R_\epsilon(y) \nabla_x g(\boldsymbol{x}, y), \quad (17)$$

$$\dot{\eta} = -Q_{y\bullet}(\boldsymbol{z} - \boldsymbol{z}_r) - \boldsymbol{p}^T \boldsymbol{f}_y(\boldsymbol{x}, y) - \boldsymbol{p}^T \boldsymbol{B}_y(\boldsymbol{x}, y)\boldsymbol{u} - \eta \left[g_y R_\epsilon + g R'_\epsilon \right]. \quad (18)$$

Here B_j denotes the j-th column of $\boldsymbol{B}$, and $Q_{x\bullet}$, $Q_{y\bullet}$ denote the corresponding block rows of Q.

Proposition 4.2 (Explicit optimal control)**.** *If $R \succ 0$, then the Hamiltonian is strictly convex in $\boldsymbol{u}$. If $U = \mathbb{R}^m$,*

$$\boldsymbol{u}_\epsilon^* = -R^{-1} \boldsymbol{B}(\boldsymbol{x}, y)^T \boldsymbol{p}. \quad (19)$$

If U is a closed convex set, then

$$\boldsymbol{u}_\epsilon^* = \mathrm{Proj}_U^R\big(-R^{-1} \boldsymbol{B}(\boldsymbol{x}, y)^T \boldsymbol{p}\big), \quad (20)$$

where $\mathrm{Proj}_U^R(w) = \arg\min_{v \in U} (v - w)^T R (v - w)$.

Proof Only two terms of H_ϵ depend on $\boldsymbol{u}$: $\mathcal{Q}(\boldsymbol{u}) = \frac{1}{2}\boldsymbol{u}^T R \boldsymbol{u} + \boldsymbol{p}^T \boldsymbol{B} \boldsymbol{u}$. Since $R \succ 0$, the Hessian $D_{uu}^2 \mathcal{Q} = R$ is positive definite, so $\mathcal{Q}$ is strictly convex and has at most one minimizer on a convex feasible set. Completing the square gives

$$\mathcal{Q}(\boldsymbol{u}) = \frac{1}{2} \left(\boldsymbol{u} + R^{-1} \boldsymbol{B}^T \boldsymbol{p} \right)^T R \left(\boldsymbol{u} + R^{-1} \boldsymbol{B}^T \boldsymbol{p} \right) - \frac{1}{2} \boldsymbol{p}^T \boldsymbol{B} R^{-1} \boldsymbol{B}^T \boldsymbol{p}.$$

The second term is independent of $\boldsymbol{u}$. If $U = \mathbb{R}^m$, the first quadratic form is minimized uniquely when its argument vanishes, yielding (19). If U is closed and convex, minimizing the first term is exactly the metric-projection problem $\min_{v \in U} (v - w)^T R (v - w)$, $w = -R^{-1} \boldsymbol{B}^T \boldsymbol{p}$. Positive definiteness of R and closed convexity of U guarantee a unique metric projection, proving (20). □

5 Optimal control on the selected invariant dynamics

Consider initial data on the invariant hyperplane S of the regularized family and a reference and terminal target that also lie on S. By Proposition 3.5, every regularized member follows the same selected generalized dynamics (10) for every $\epsilon > 0$. This is an exact statement about the regularized family, not a claim of classical solvability of the original implicit equation on the impasse set. Let $x_r(t)$ be the tangential reference and define

$$J_s(\boldsymbol{u}) = \frac{1}{2}(\boldsymbol{x}(T) - \boldsymbol{x}_T)^T Q_{sT} (\boldsymbol{x}(T) - \boldsymbol{x}_T) + \frac{1}{2} \int_0^T (\boldsymbol{x} - x_r)^T Q_s (\boldsymbol{x} - x_r)\, dt + \frac{1}{2} \int_0^T \boldsymbol{u}^T R \boldsymbol{u}\, dt.$$

The selected on-manifold Hamiltonian is $H_s = \frac{1}{2}(\boldsymbol{x} - x_r)^T Q_s (\boldsymbol{x} - x_r) + \frac{1}{2}\boldsymbol{u}^T R \boldsymbol{u} + \boldsymbol{p}^T \big(\boldsymbol{f}_s(\boldsymbol{x}) + \boldsymbol{B}_s(\boldsymbol{x}) \boldsymbol{u} \big)$. Hence

$$\dot{\boldsymbol{x}} = \boldsymbol{f}_s(\boldsymbol{x}) + \boldsymbol{B}_s(\boldsymbol{x}) \boldsymbol{u}, \quad (21)$$

$$\dot{\boldsymbol{p}} = -Q_s(\boldsymbol{x} - x_r) - D\boldsymbol{f}_s(\boldsymbol{x})^T\boldsymbol{p} - \sum_{j=1}^{m} u_j DB_{s,j}(\boldsymbol{x})^T\boldsymbol{p}, \tag{22}$$

$$\boldsymbol{u}_s^* = \mathrm{Proj}_U^R\big(-R^{-1}\boldsymbol{B}_s(\boldsymbol{x})^T\boldsymbol{p}\big)\,. \tag{23}$$

Theorem 5.1 (Exact equivalence of the on-manifold optimal-control problems)**.** *Fix $\epsilon > 0$. Assume that the regularized state equation has a unique solution on $[0,T]$ for every admissible control. Let $\boldsymbol{z}(0) = (\boldsymbol{x}_0, y^*)$, $\boldsymbol{z}_r(t) = (\boldsymbol{x}_r(t), y^*)$, $\boldsymbol{z}_T = (\boldsymbol{x}_T, y^*)$. Let Q_s and Q_{sT} denote the tangential principal blocks of Q and Q_T, respectively. Then, for every admissible control $\boldsymbol{u}$,*

(i) the regularized trajectory remains on S and satisfies (21)*;*
(ii) the full regularized cost and selected cost coincide, $J_\epsilon(\boldsymbol{u}) = J_s(\boldsymbol{u})$;
(iii) the optimal values and the sets of minimizing controls coincide;
(iv) the tangential part of the regularized Pontryagin system is exactly (21)–(23) *and is independent of ϵ.*

Thus the selected lower-dimensional optimal-control problem is an exact invariant subproblem of every regularized problem, rather than an asymptotic $\epsilon \to 0$ approximation.

Proof Fix an arbitrary admissible control $\boldsymbol{u}$. Proposition 3.5 applies because $y(0) = y^*$, and therefore $y_\epsilon(t) = y^*$ $(0 \le t \le T)$. Substitution into the tangential state equation gives

$$\dot{\boldsymbol{x}}_\epsilon = \boldsymbol{f}(\boldsymbol{x}_\epsilon, y^*) + \boldsymbol{B}(\boldsymbol{x}_\epsilon, y^*)\boldsymbol{u} = \boldsymbol{f}_s(\boldsymbol{x}_\epsilon) + \boldsymbol{B}_s(\boldsymbol{x}_\epsilon)\boldsymbol{u}.$$

Thus the regularized control-to-state map on its invariant hyperplane is exactly the selected lower-dimensional control-to-state map, proving (i).

For the cost, write the symmetric matrices in block form,

$$Q = \begin{bmatrix} Q_s & q \\ q^T & q_y \end{bmatrix},\; Q_T = \begin{bmatrix} Q_{sT} & q_T \\ q_T^T & q_{Ty} \end{bmatrix}.$$

Since both the trajectory and the reference lie on S,

$$\boldsymbol{z}(t) - \boldsymbol{z}_r(t) = \begin{bmatrix} \boldsymbol{x}(t) - \boldsymbol{x}_r(t) \\ 0 \end{bmatrix}.$$

Hence $(\boldsymbol{z} - \boldsymbol{z}_r)^T Q(\boldsymbol{z} - \boldsymbol{z}_r) = (\boldsymbol{x} - \boldsymbol{x}_r)^T Q_s(\boldsymbol{x} - \boldsymbol{x}_r)$; the normal quadratic term and both cross terms vanish exactly. The same calculation at T gives $(\boldsymbol{z}(T) - \boldsymbol{z}_T)^T Q_T(\boldsymbol{z}(T) - \boldsymbol{z}_T) = (\boldsymbol{x}(T) - \boldsymbol{x}_T)^T Q_{sT}(\boldsymbol{x}(T) - \boldsymbol{x}_T)$. The control penalty is identical in the two problems, so $J_\epsilon(\boldsymbol{u}) = J_s(\boldsymbol{u})$, proving (ii).

The admissible control class is the same in both problems, and the equality in (ii) holds for every admissible control. Consequently $\inf_{\boldsymbol{u}} J_\epsilon(\boldsymbol{u}) = \inf_{\boldsymbol{u}} J_s(\boldsymbol{u})$. Moreover, a control minimizes one functional if and only if it minimizes the other. Hence both the optimal values and the complete sets of minimizers coincide, proving (iii).

It remains to compare the PMP systems. On S, the tangential state equation has already been shown to coincide. In the tangential adjoint equation (17), the only term involving the normal costate is $-\eta R_\epsilon(y)\nabla_x g(\boldsymbol{x}, y)$. Because $R_\epsilon(y^*) = 0$, this term vanishes identically on every on-manifold extremal. Furthermore, $Q_{x\bullet}(\boldsymbol{z} - \boldsymbol{z}_r) = Q_s(\boldsymbol{x} - \boldsymbol{x}_r)$, and evaluation of $D_x\boldsymbol{f}$ and $D_x B_j$ at $y = y^*$ gives $D\boldsymbol{f}_s$ and $DB_{s,j}$. Therefore (17) becomes exactly (22). At the terminal time, $\boldsymbol{p}(T) = Q_{sT}(\boldsymbol{x}(T) - \boldsymbol{x}_T)$, because the normal terminal deviation is

zero. Finally, the $\boldsymbol{u}$-dependent part of the Hamiltonian on S is $\frac{1}{2}\boldsymbol{u}^T R\boldsymbol{u} + \boldsymbol{p}^T \boldsymbol{B}_s(\boldsymbol{x})\boldsymbol{u}$, so Proposition 4.2 yields precisely (23). The normal costate η may be nonzero and may satisfy a stiff scalar equation, but it is multiplied by $R_\epsilon(y^*) = 0$ in the tangential adjoint and never enters the Hamiltonian derivative with respect to $\boldsymbol{u}$. This proves (iv). □

Remark 5.2 (Scope of the exact equivalence). Theorem 5.1 concerns the on-manifold regulation problem used for suppression and exit avoidance. It deliberately avoids any unsupported limiting statement for off-manifold adjoints. Optimal shaping of a complete relaxation cycle through ejection and re-entry is a distinct hybrid optimal-control problem; at such events the adjoint may require jump/transversality conditions. Those event-sensitive conditions are not needed when the controller keeps the trajectory inside $\mathcal{D}$ and makes the singular exit unreachable.

5.1 Hamilton–Jacobi–Bellman characterization

Let $V(t, \boldsymbol{x})$ denote the value function for the selected on-manifold problem. In a region in which V is differentiable, it satisfies

$$-V_t = \min_{\boldsymbol{u}\in U} \left\{ \frac{1}{2}(\boldsymbol{x} - x_r)^T Q_s(\boldsymbol{x} - x_r) + \frac{1}{2}\boldsymbol{u}^T R\boldsymbol{u} + \nabla_{\boldsymbol{x}} V^T(\boldsymbol{f}_s + \boldsymbol{B}_s\boldsymbol{u}) \right\}. \tag{24}$$

For $U = \mathbb{R}^m$, the minimizing feedback is $\boldsymbol{u}^*(t, \boldsymbol{x}) = -R^{-1}\boldsymbol{B}_s(\boldsymbol{x})^T \nabla_{\boldsymbol{x}} V(t, \boldsymbol{x})$. Along a smooth optimal extremal, $\boldsymbol{p} = \nabla_{\boldsymbol{x}} V$, so the PMP and HJB descriptions are consistent.

Corollary 5.3 (Exact restriction of the value function)**.** *Let $V_\epsilon(t, \boldsymbol{x}, y)$ denote the value function of the regularized finite-horizon problem and let $V_s(t, \boldsymbol{x})$ denote the value function of the selected problem, with on-manifold reference and target as in Theorem 5.1. Then $V_\epsilon(t, \boldsymbol{x}, y^*) = V_s(t, \boldsymbol{x})$ for every $\epsilon > 0$. Wherever both sides are differentiable, $\nabla_x V_\epsilon(t, \boldsymbol{x}, y^*) = \nabla_x V_s(t, \boldsymbol{x})$, and the corresponding tangential HJB feedback is independent of ϵ.*

Proof Fix a starting time t, a tangential state $\boldsymbol{x}$, and an arbitrary admissible control on $[t, T]$. Starting from $(\boldsymbol{x}, y^*)$, Proposition 3.5 forces the regularized trajectory to remain on S. Theorem 5.1 then shows that this control produces exactly the same tangential state trajectory and exactly the same cost-to-go in the regularized and selected problems. Since this equality holds control by control over the same admissible class, taking the infimum yields $V_\epsilon(t, \boldsymbol{x}, y^*) = V_s(t, \boldsymbol{x})$. If both value functions are differentiable with respect to $\boldsymbol{x}$, differentiation of this identity along S gives the gradient equality. Substituting the common tangential gradient into the strictly convex HJB minimization gives the same feedback in both problems, and no ϵ-dependence remains. □

5.2 Off-manifold consistency of costs, optimal values, and minimizers

The exact equivalence above concerns initial data on S. The normal-tube estimate also permits a quantitative optimal-control comparison for initial states at distance

$O(\epsilon)$ from the selected hyperplane. Let

$$\ell(t,\boldsymbol{z},\boldsymbol{u}) = \frac{1}{2}(\boldsymbol{z}-\boldsymbol{z}_r)^T Q(\boldsymbol{z}-\boldsymbol{z}_r) + \frac{1}{2}\boldsymbol{u}^T R\boldsymbol{u},\ \Phi(\boldsymbol{z}) = \frac{1}{2}(\boldsymbol{z}-\boldsymbol{z}_T)^T Q_T(\boldsymbol{z}-\boldsymbol{z}_T).$$

On every compact state set these functions are Lipschitz in $\boldsymbol{z}$, uniformly for $\boldsymbol{u} \in U$.

For the next result, let $\mathcal{U}_K$ be an admissible control class for which all selected trajectories issued from the same tangential initial state remain in a common compact set $K_0 \Subset K \Subset \mathcal{D}_\delta$ on $[0,T]$. Thus the constants in Theorem 3.2 can be chosen uniformly for $\boldsymbol{u} \in \mathcal{U}_K$.

Theorem 5.4 (Uniform off-manifold cost consistency)**.** *Assume the hypotheses above, let $\boldsymbol{x}_\epsilon(0) = \boldsymbol{x}_s(0) = \boldsymbol{x}_0$, $e_0 := y_\epsilon(0) - y^*$, $|e_0| \le r\epsilon$. and let the reference and terminal target lie on S. Then there are constants $C_J > 0$ and $\epsilon_1 > 0$, independent of $\boldsymbol{u} \in \mathcal{U}_K$ and $0 < \epsilon \le \epsilon_1$, such that*

$$|J_\epsilon(\boldsymbol{u}) - J_s(\boldsymbol{u})| \le C_J \epsilon^2 |e_0|. \tag{25}$$

Consequently, if $|e_0| \le C_0\epsilon$, then $\sup_{\boldsymbol{u}\in\mathcal{U}_K} |J_\epsilon(\boldsymbol{u}) - J_s(\boldsymbol{u})| = O(\epsilon^3)$.

Proof For a fixed $\boldsymbol{u} \in \mathcal{U}_K$, let $\Delta_x(t) = \boldsymbol{x}_\epsilon(t) - \boldsymbol{x}_s(t)$, $e(t) = y_\epsilon(t) - y^*$. Uniformity of the compact sets and of U implies that the constants c, C_T in Theorem 3.2 can be chosen independently of $\boldsymbol{u} \in \mathcal{U}_K$. Hence $\sup_{0\le t\le T} \|\Delta_x(t)\| \le C_T\epsilon^2|e_0|$, $|e(t)| \le |e_0|e^{-ct/\epsilon^2}$. Let L_ℓ, L_Φ be state-Lipschitz constants for ℓ and Φ on the common compact tube. Since the same control is used in both problems, the control-penalty terms cancel when the running costs are subtracted. Using $\|\boldsymbol{z}_\epsilon(t) - \boldsymbol{z}_s(t)\| \le \|\Delta_x(t)\| + |e(t)|$, we obtain

$$|J_\epsilon(\boldsymbol{u}) - J_s(\boldsymbol{u})| \le L_\Phi\big(\|\Delta_x(T)\| + |e(T)|\big) + L_\ell \int_0^T \big(\|\Delta_x(t)\| + |e(t)|\big)\, dt.$$

The tangential contribution satisfies $\int_0^T \|\Delta_x(t)\|dt \le TC_T\epsilon^2|e_0|$, and the normal contribution obeys $\int_0^T |e(t)|dt \le |e_0| \int_0^T e^{-ct/\epsilon^2}dt \le \frac{\epsilon^2}{c}|e_0|$. At the terminal time, $\|\Delta_x(T)\| \le C_T\epsilon^2|e_0|$, $|e(T)| \le |e_0|e^{-cT/\epsilon^2}$. Therefore

$$|J_\epsilon - J_s| \le \left[L_\Phi C_T + L_\ell\left(TC_T + \frac{1}{c}\right)\right]\epsilon^2|e_0| + L_\Phi|e_0|e^{-cT/\epsilon^2}.$$

Since the exponential is super-algebraically small, after reducing ϵ_1 if necessary one has $e^{-cT/\epsilon^2} \le \epsilon^2$ $(0 < \epsilon \le \epsilon_1)$. Absorbing the terminal exponential term into the same constant gives (25). If $|e_0| \le C_0\epsilon$, the right-hand side is $O(\epsilon^3)$, uniformly over $\mathcal{U}_K$. □

Corollary 5.5 (Off-manifold convergence of optimal values away from terminal time)**.** *Fix $\tau > 0$. Let $0 \le t \le T - \tau$, and let $V_\epsilon^K(t,\boldsymbol{x},y^*+e_0)$ and $V_s^K(t,\boldsymbol{x})$ denote the value functions obtained by minimizing over the same safety-core admissible class on the remaining interval $[t,T]$. Assume that the hypotheses of Theorem 5.4 hold uniformly for starting times $t \in [0,T-\tau]$. Then there exist constants $C_{V,\tau} > 0$ and $\epsilon_\tau > 0$, independent of t, ϵ, and the admissible control, such that*

$$\big|V_\epsilon^K(t,\boldsymbol{x},y^*+e_0) - V_s^K(t,\boldsymbol{x})\big| \le C_{V,\tau}\epsilon^2|e_0|,\ 0 < \epsilon \le \epsilon_\tau. \tag{26}$$

In particular, if $|e_0| = O(\epsilon)$, then, uniformly for $t \in [0,T-\tau]$, $V_\epsilon^K(t,\boldsymbol{x},y^*+e_0) = V_s^K(t,\boldsymbol{x}) + O(\epsilon^3)$. For any single fixed starting time $t < T$, the same estimate follows by taking any $\tau \in (0,T-t]$.

Proof Fix $\tau > 0$ and $t \in [0, T-\tau]$. The remaining horizon satisfies $T - t \geq \tau > 0$. Apply the proof of Theorem 5.4 on the shifted interval $[t, T]$. By the assumed uniform safety-core hypothesis, the normal-tube constants can be chosen independently of $t \in [0, T-\tau]$. In particular, $|e(s)| \leq |e_0| \exp\Big(-\frac{c(s-t)}{\epsilon^2}\Big)$, $t \leq s \leq T$, and $\sup_{s\in[t,T]} \|\boldsymbol{x}_\epsilon(s) - \boldsymbol{x}_s(s)\| \leq C_{T,\tau}\epsilon^2|e_0|$. The integral normal contribution satisfies $\int_t^T |e(s)|\, ds \leq \frac{\epsilon^2}{c}|e_0|$, while the terminal normal displacement obeys

$$|e(T)| \leq |e_0| \exp\left(-\frac{c(T-t)}{\epsilon^2}\right) \leq |e_0| \exp\Big(-\frac{c\tau}{\epsilon^2}\Big).$$

Because $\tau > 0$ is fixed, $\exp\big(-\frac{c\tau}{\epsilon^2}\big) = o(\epsilon^N)$ for every $N > 0$. Hence, after reducing ϵ_τ if necessary, $\exp\big(-\frac{c\tau}{\epsilon^2}\big) \leq \epsilon^2$ $(0 < \epsilon \leq \epsilon_\tau)$, uniformly with respect to $t \in [0, T-\tau]$. Therefore the same Lipschitz-cost argument as in Theorem 5.4 gives $\sup_{\boldsymbol{u}\in\mathcal{U}_K} |J_{\epsilon,t}(\boldsymbol{u}) - J_{s,t}(\boldsymbol{u})| \leq C_{V,\tau}\epsilon^2|e_0|$, where $J_{\epsilon,t}$ and $J_{s,t}$ denote the corresponding costs-to-go from time t.

For arbitrary real-valued functionals F and G on the same admissible set, $|\inf F - \inf G| \leq \sup|F - G|$. Applying this inequality to the two costs-to-go proves (26). If $|e_0| = O(\epsilon)$, the right-hand side is $O(\epsilon^3)$, uniformly for $t \in [0, T-\tau]$.

The restriction $t \leq T - \tau$ is essential for a uniform estimate: if $t \to T$ together with ϵ, the remaining horizon can be comparable with or smaller than the normal boundary-layer time scale $O(\epsilon^2)$, and the terminal normal discrepancy need not be $O(\epsilon^2|e_0|)$. For each fixed $t < T$, however, one may choose a positive $\tau \leq T - t$, so the estimate remains valid pointwise for every starting time strictly before the terminal time. □

Proposition 5.6 (Consistency of minimizers under compactness)**.** *Let $\mathcal{U}_K$ be sequentially compact in a metrizable topology τ, assume J_s is τ-lower semicontinuous and has a unique minimizer $\boldsymbol{u}_s^*$, and let $\boldsymbol{u}_\epsilon^*$ be a minimizer of J_ϵ over $\mathcal{U}_K$. If the uniform estimate of Theorem 5.4 holds, then $\boldsymbol{u}_\epsilon^* \longrightarrow \boldsymbol{u}_s^*$ in τ as $\epsilon \downarrow 0$.*

Proof Let $\delta_\epsilon = \sup_{\boldsymbol{u}\in\mathcal{U}_K} |J_\epsilon(\boldsymbol{u}) - J_s(\boldsymbol{u})| \longrightarrow 0$. Optimality of $\boldsymbol{u}_\epsilon^*$ for J_ϵ gives $J_\epsilon(\boldsymbol{u}_\epsilon^*) \leq J_\epsilon(\boldsymbol{u}_s^*)$. Adding and subtracting J_s and using the uniform error bound yields $J_s(\boldsymbol{u}_\epsilon^*) \leq J_s(\boldsymbol{u}_s^*) + 2\delta_\epsilon$. Take any sequence $\epsilon_j \downarrow 0$. Sequential compactness gives a subsequence, not relabeled, with $\boldsymbol{u}_{\epsilon_j}^* \xrightarrow{\tau} \bar{\boldsymbol{u}}$. Lower semicontinuity then implies $J_s(\bar{\boldsymbol{u}}) \leq \liminf_{j\to\infty} J_s(\boldsymbol{u}_{\epsilon_j}^*) \leq J_s(\boldsymbol{u}_s^*)$. Thus $\bar{\boldsymbol{u}}$ is a minimizer of J_s; uniqueness forces $\bar{\boldsymbol{u}} = \boldsymbol{u}_s^*$. To conclude convergence of the full family, let d_τ be a metric generating τ. If convergence failed, there would be $\eta > 0$ and a sequence $\epsilon_j \downarrow 0$ with $d_\tau(\boldsymbol{u}_{\epsilon_j}^*, \boldsymbol{u}_s^*) \geq \eta$. Sequential compactness would provide a convergent subsequence, and the preceding argument would force its limit to be $\boldsymbol{u}_s^*$, a contradiction. Hence the full family converges to $\boldsymbol{u}_s^*$ in τ. □

Remark 5.7. Proposition 5.6 is deliberately conditional: it does not claim compactness or uniqueness for every nonlinear control problem. Its role is to show that the uniform $O(\epsilon^3)$ cost consistency established above immediately yields optimizer consistency whenever the usual compactness and uniqueness hypotheses are available.

6 Exit-constrained optimal control and real-time safety filtering

The exit manifold is not merely a geometric boundary: loss of the condition $h > 0$ removes normal attraction and activates the singular transition. We therefore

introduce the *exit-constrained selected optimal-control problem (OCP)*

$$\begin{aligned} &\min_{\boldsymbol{u}(\cdot)} \Phi(\boldsymbol{x}(T)) + \int_0^T L(t, \boldsymbol{x}(t), \boldsymbol{u}(t))\, dt, \\ \text{subject to } &\dot{\boldsymbol{x}} = \boldsymbol{f}_s(\boldsymbol{x}) + \boldsymbol{B}_s(\boldsymbol{x})\boldsymbol{u}, \\ &\boldsymbol{u}(t) \in U, \\ &h(\boldsymbol{x}(t)) - \delta \geq 0,\ 0 \leq t \leq T. \end{aligned} \tag{27}$$

The path constraint is part of the horizon optimization itself. In the general smooth theory its multiplier is represented by a nonnegative measure, or equivalently by a bounded-variation modification of the costate, supported on the active set $h = \delta$ [18–20]. On an interior arc where $h > \delta$, the ordinary selected on-manifold PMP stated above is recovered.

Corollary 6.1 (Exact equivalence with tangential path constraints)**.** *Assume the hypotheses of Theorem 5.1. Impose on the regularized and selected problems the same collection of path constraints $c_j(t, \boldsymbol{x}(t)) \geq 0$, $j = 1, \ldots, N_c$, that depend only on the tangential state and time, together with the same control constraint $\boldsymbol{u}(t) \in U$. Then, for every $\epsilon > 0$, the two on-manifold problems have exactly the same feasible controls, the same cost for every feasible control, the same constrained optimal value, and the same set of constrained minimizers. In particular, this statement applies to the exit constraint $h(\boldsymbol{x}(t)) - \delta \geq 0$ in* (27)*.*

Proof For any admissible control and on-manifold initial state, Proposition 3.5 gives the same tangential trajectory $\boldsymbol{x}(\cdot)$ in the regularized and selected systems. Therefore every tangential path constraint $c_j(t, \boldsymbol{x}(t)) \geq 0$ is satisfied in one problem if and only if it is satisfied in the other. Hence the feasible control sets coincide. Theorem 5.1 gives equality of the costs control by control on this common feasible set. Taking infima proves equality of constrained optimal values, and equality of the minimizing-control sets follows immediately. □

Remark 6.2 (State constraint versus singular exit). The inequality $h(\boldsymbol{x}) \geq \delta$ is not an arbitrary engineering bound. It prescribes a geometric margin from the loss-of-attraction set of the regularized singular dynamics. In a state-constrained PMP, the associated multiplier therefore has a direct interpretation as the marginal cost, or shadow price, of preventing accessibility of the singular ejection mechanism.

For a regular relative-degree-one boundary arc one can state the geometry explicitly. Let $a(\boldsymbol{x}) := L_{\boldsymbol{B}_s} h(\boldsymbol{x}) \in \mathbb{R}^{1\times m}$, $b(\boldsymbol{x}) := -L_{\boldsymbol{f}_s} h(\boldsymbol{x})$.

Proposition 6.3 (Optimal tangential control on a regular exit boundary)**.** *Assume $a(\boldsymbol{x}) = L_{\boldsymbol{B}_s} h(\boldsymbol{x}) \neq 0$ on an active boundary arc $h(\boldsymbol{x}) = \delta$, and assume the resulting boundary control lies in* $\operatorname{int} U$*, so that no input inequality is active. Let $\boldsymbol{p}$ denote the appropriate boundary-arc costate, including the state-constraint multiplier in a standard state-constrained PMP formulation, and suppose the control-dependent Hamiltonian is $\frac{1}{2}\boldsymbol{u}^T R\boldsymbol{u} + \boldsymbol{p}^T \boldsymbol{B}_s \boldsymbol{u}$, $R \succ 0$. Then tangency requires $a(\boldsymbol{x})\boldsymbol{u} = b(\boldsymbol{x})$, and*

the Hamiltonian-minimizing boundary control is

$$\boldsymbol{u}_b = \boldsymbol{u}_0 + R^{-1}a^T \frac{b - a\boldsymbol{u}_0}{aR^{-1}a^T},\ \boldsymbol{u}_0 = -R^{-1}\boldsymbol{B}_s^T\boldsymbol{p}. \tag{28}$$

Thus the state constraint projects the unconstrained Hamiltonian minimizer onto the tangency hyperplane in the R-metric.

Proof On an interior portion of a regular active boundary arc, the state remains on $h(\boldsymbol{x}) = \delta$. Differentiating this equality along the selected on-manifold dynamics gives $0 = \dot{h} = L_{\boldsymbol{f}_s}h + L_{\boldsymbol{B}_s}h\,\boldsymbol{u}$. With $a = L_{\boldsymbol{B}_s}h$ and $b = -L_{\boldsymbol{f}_s}h$, this is exactly the affine tangency condition $a\boldsymbol{u} = b$.

Complete the square in the control-dependent Hamiltonian: $\frac{1}{2}\boldsymbol{u}^T R\boldsymbol{u} + \boldsymbol{p}^T\boldsymbol{B}_s\boldsymbol{u} = \frac{1}{2}(\boldsymbol{u} - \boldsymbol{u}_0)^T R(\boldsymbol{u} - \boldsymbol{u}_0) + \text{constant}$, where $\boldsymbol{u}_0 = -R^{-1}\boldsymbol{B}_s^T\boldsymbol{p}$. Thus the boundary control solves $\min_{\boldsymbol{u}}\ \frac{1}{2}(\boldsymbol{u} - \boldsymbol{u}_0)^T R(\boldsymbol{u} - \boldsymbol{u}_0)$ subject to $a\boldsymbol{u} = b$. Introduce a scalar Lagrange multiplier μ: $\mathcal{L}_b(\boldsymbol{u}, \mu) = \frac{1}{2}(\boldsymbol{u} - \boldsymbol{u}_0)^T R(\boldsymbol{u} - \boldsymbol{u}_0) + \mu(a\boldsymbol{u} - b)$. Stationarity with respect to $\boldsymbol{u}$ gives $R(\boldsymbol{u} - \boldsymbol{u}_0) + a^T\mu = 0$, so $\boldsymbol{u} = \boldsymbol{u}_0 - R^{-1}a^T\mu$. Substitution into $a\boldsymbol{u} = b$ yields $\mu = \frac{a\boldsymbol{u}_0 - b}{aR^{-1}a^T}$. Since $R \succ 0$ and $a \neq 0$, the denominator $aR^{-1}a^T$ is strictly positive. Inserting μ into the stationary control gives (28). Strict convexity of the quadratic objective makes this stationary point the unique minimizer. The assumption $\boldsymbol{u}_b \in \operatorname{int} U$ ensures that no additional input-bound Karush–Kuhn–Tucker (KKT) multipliers are required. □

Remark 6.4 (When the tangency control saturates). If $\boldsymbol{u}_b$ in (28) fails to lie in U, the hypothesis of Proposition 6.3 is violated and an input-bound multiplier must be adjoined to the state-constraint multiplier. For a scalar control with box constraint $U = [-u_{\max}, u_{\max}]$, as used throughout the numerical examples below, the resolution is elementary: minimizing $\frac{1}{2}(u - u_0)^T R(u - u_0)$ subject to $au = b$ and $|u| \leq u_{\max}$ still returns u_b from (28) whenever $|u_b| \leq u_{\max}$, because the box constraint is then inactive at the unique equality-constrained minimizer. If instead $|u_b| > u_{\max}$, the two constraints are jointly infeasible – no admissible scalar control can hold $au = b$ exactly – so the state cannot slide along $h = \delta$; it can only cross or touch the boundary transversally, and a genuine boundary arc requires either relaxing the margin δ or increasing $u_{\max}$. At the boundary point used in Section 8 below, $u_b = 0$ lies well inside $|u| \leq 3$, so this degeneracy does not arise there.

If $L_{\boldsymbol{B}_s}h = 0$, the first control-dependent tangency condition occurs at a higher derivative. For relative degree two, an active boundary arc satisfies $h = \delta$, $\dot{h} = 0$, and $\ddot{h} = 0$, with the last equation affine in the control under the standard regularity condition.

For online protection we retain a control-barrier safety layer. If $L_{\boldsymbol{B}_s}h \neq 0$, a relative-degree-one control barrier function (CBF) condition is

$$L_{\boldsymbol{f}_s}h + L_{\boldsymbol{B}_s}h\boldsymbol{u} \geq -\alpha(h - \delta). \tag{29}$$

Given a nominal command $\boldsymbol{u}_{\text{nom}}$, the filter

$$\min_{\boldsymbol{u} \in U} \frac{1}{2}(\boldsymbol{u} - \boldsymbol{u}_{\text{nom}})^T R(\boldsymbol{u} - \boldsymbol{u}_{\text{nom}}) \text{ subject to (29)}$$

preserves the nominal command whenever it is already safe. When the filter is active, however, it minimizes only the instantaneous R-metric modification and is not, in general, the global minimizer of the original horizon cost.

For relative degree two we use a high-order control barrier function (HOCBF) construction $\psi_0 = h - \delta, \psi_1 = \dot{\psi}_0 + k_1\psi_0$, with $\dot{\psi}_1 + k_2\psi_1 \geq 0, k_1, k_2 > 0$. Forward invariance requires not only feasibility of this affine input inequality but also compatible initial conditions

$$\psi_0(\boldsymbol{x}(0)) \geq 0,\ \psi_1(\boldsymbol{x}(0)) \geq 0. \tag{30}$$

The required comparison step can be stated directly as follows.

Proposition 6.5 (Forward invariance of the relative-degree-two barrier cascade)**.** *Assume that a closed-loop trajectory exists on $[0, T]$, that ψ_0 and ψ_1 are absolutely continuous along it, and that, almost everywhere, $\psi_1 = \dot{\psi}_0 + k_1\psi_0$, $\dot{\psi}_1 + k_2\psi_1 \geq 0$, $k_1, k_2 > 0$. If (30) holds, then $\psi_1(t) \geq 0$ and $\psi_0(t) \geq 0$ for every $t \in [0, T]$. Consequently $h(\boldsymbol{x}(t)) \geq \delta$ throughout the interval. Thus, provided the HOCBF input inequality and the actuator constraints remain jointly feasible, the admissible high-order barrier set is forward invariant [26, 27].*

Proof Multiplication of $\dot{\psi}_1 + k_2\psi_1 \geq 0$ by the integrating factor $e^{k_2 t}$ gives $\frac{d}{dt}\left(e^{k_2 t}\psi_1(t)\right) \geq 0$ almost everywhere. Hence $\psi_1(t) \geq e^{-k_2 t}\psi_1(0) \geq 0$. Using $\psi_1 = \dot{\psi}_0 + k_1\psi_0$ therefore yields $\dot{\psi}_0 + k_1\psi_0 \geq 0$. A second integrating-factor argument gives $\psi_0(t) \geq e^{-k_1 t}\psi_0(0) \geq 0$. Since $\psi_0 = h - \delta$, the exit margin remains nonnegative on $[0, T]$. □

7 Local optimal stabilization inside the sliding domain

Let $\bar{x} \in \mathcal{D}$ satisfy $\boldsymbol{f}_s(\bar{x}) = 0$, set $\xi = \boldsymbol{x} - \bar{x}$, and write

$$\dot{\xi} = A\xi + B\boldsymbol{u} + O(|\xi|^2 + |\xi||\boldsymbol{u}|),\ A = D\boldsymbol{f}_s(\bar{x}),\ B = \boldsymbol{B}_s(\bar{x}). \tag{31}$$

For the linearized system consider the unconstrained infinite-horizon linear-quadratic regulator (LQR) problem with cost

$$J_{\mathrm{LQR}} = \frac{1}{2}\int_0^\infty (\xi^T Q\xi + \boldsymbol{u}^T R\boldsymbol{u})\, dt,\ Q \succeq 0,\ R \succ 0. \tag{32}$$

If the original problem has a bounded input set U, assume $0 \in \operatorname{int} U$; the local nonlinear conclusion below is then understood on a sufficiently small neighborhood in which the unconstrained feedback $-K\xi$ remains in U.

Theorem 7.1 (Local LQR stabilization)**.** *Assume (A, B) is stabilizable and $(Q^{1/2}, A)$ is detectable. Let $P = P^T \succeq 0$ be the stabilizing solution of*

$$A^T P + PA - PBR^{-1}B^T P + Q = 0. \tag{33}$$

Then $\boldsymbol{u} = -K\xi$, $K = R^{-1}B^T P$, minimizes (32) for the linearized sliding system and makes $A - BK$ Hurwitz. Consequently the equilibrium of the nonlinear closed loop is locally asymptotically stable by the Lyapunov indirect method. Moreover, for any $W_L \succ 0$, the Lyapunov equation $(A - BK)^T P_L + P_L(A - BK) = -W_L$ has a unique solution $P_L \succ 0$; sufficiently small sublevel sets of $V_L = \xi^T P_L \xi$ are positively invariant. If such a sublevel set is contained in $\mathcal{D}$, the local ejection mechanism is inaccessible from that set.

Proof Under stabilizability of (A, B), detectability of $(Q^{1/2}, A)$, and $R \succ 0$, standard continuous-time LQR theory [28] gives a unique stabilizing symmetric solution $P \succeq 0$. The associated gain $K = R^{-1}B^T P$ makes $A_c := A - BK$ Hurwitz and gives the unique stabilizing linear-quadratic feedback. Standard completion-of-squares or dynamic-programming arguments then show that this feedback minimizes (32) for the linearized system.

Now write the nonlinear closed loop as $\dot{\xi} = A_c\xi + r_c(\xi)$, $\frac{\|r_c(\xi)\|}{\|\xi\|} \to 0$ as $\xi \to 0$. Because A_c is Hurwitz, the Lyapunov indirect theorem [29] already gives local asymptotic stability. For the invariant-set statement, fix any $W_L \succ 0$. The Lyapunov equation $A_c^T P_L + P_L A_c = -W_L$ has the integral representation $P_L = \int_0^\infty e^{A_c^T t} W_L e^{A_c t}\, dt$, which proves both existence and positive definiteness of P_L. Along the nonlinear closed loop, $\dot{V}_L = -\xi^T W_L \xi + 2\xi^T P_L r_c(\xi)$. For every $\eta > 0$, the higher-order property of r_c gives a neighborhood in which $\|r_c(\xi)\| \le \eta\|\xi\|$. Hence $\dot{V}_L \le -\lambda_{\min}(W_L)\|\xi\|^2 + 2\|P_L\|\eta\|\xi\|^2$. Choose $\eta < \lambda_{\min}(W_L)/(2\|P_L\|)$. Then $\dot{V}_L < 0$ for every nonzero ξ in a sufficiently small neighborhood. Because V_L is positive definite, a sufficiently small sublevel set $\{V_L \le \rho\}$ lies inside this neighborhood and is positively invariant by the standard Lyapunov sublevel-set argument. If its closure is also contained in $\mathcal{D}$, no trajectory starting in the sublevel set can reach $\Sigma = \partial\mathcal{D}$, proving the final claim. □

Theorem 7.1 separates two notions that must not be conflated: CARE supplies linear-quadratic optimality, while nonlinear positive invariance requires an additional Lyapunov estimate. In the main example below the latter estimate is computed explicitly rather than being left as an existence statement.

8 Three-dimensional Duffing–Rayleigh example

8.1 Controlled model

Consider

$$\begin{cases} \dot{x}_1 = x_2, \\ \dot{x}_2 = \alpha\big(\psi(y) - kx_1^3\big) - D(x_1)x_2 + u, \\ \varphi(y)\dot{y} = \beta(y - x_1). \end{cases} \tag{34}$$

where $\psi(y) = R_0 - r(y - y^*)^2$, $\varphi(y) = -2r(y - y^*)$, $D(x_1) = \mu[(x_1 - x_{10})^2 - \rho_D^2]$. with $x_{10} = (R_0/k)^{1/3}$. We use $\alpha = \beta = 1$, $k = 0.5$, $R_0 = 4$, $r = 0.5$, $y^* = 3$, $\mu = 0.15$, $\rho_D = 1.5$. so $x_{10} = 2$. Since $\varphi'(y^*) = -1$, $a = 1$, and $\mathcal{D} = \{x_1 < 3\}$, $\Sigma = \{x_1 = 3, y = 3\}$. The controlled sliding dynamics is

$$\begin{cases} \dot{x}_1 = x_2, \\ \dot{x}_2 = 4 - 0.5x_1^3 - D(x_1)x_2 + u. \end{cases} \tag{35}$$

The point $\bar{x} = (2, 0)$ is a sliding equilibrium. The uncontrolled Jacobian is

$$A = \begin{bmatrix} 0 & 1 \\ -6 & 0.3375 \end{bmatrix},\ B = \begin{bmatrix} 0 \\ 1 \end{bmatrix}. \tag{36}$$

Its eigenvalues are approximately $\lambda_{1,2} = 0.16875 \pm 2.44367i$, so the equilibrium is an unstable focus and nearby trajectories are driven outward toward the exit boundary.

8.2 LQR design

Choose

$$Q = \begin{bmatrix} 10 & 0 \\ 0 & 2 \end{bmatrix}, \; R = 0.5.$$

The stabilizing solution of (33) is

$$P \approx \begin{bmatrix} 10.96878 & 0.741657 \\ 0.741657 & 1.499214 \end{bmatrix},$$

and therefore

$$K = R^{-1}B^T P \approx \begin{bmatrix} 1.483315 & 2.998428 \end{bmatrix}.$$

The feedback is

$$u = -1.483315(x_1 - 2) - 2.998428x_2. \tag{37}$$

The closed-loop linearized eigenvalues are $\lambda_{1,2}^{\mathrm{cl}} \approx -1.33046 \pm 2.39023i$, which establishes a substantial stability margin relative to the uncontrolled unstable focus.

For an actuator bound $|u| \le u_{\max}$, the natural constrained approximation is

$$u = \mathrm{sat}_{[-u_{\max}, u_{\max}]}\big[-1.483315(x_1 - 2) - 2.998428x_2\big]. \tag{38}$$

which is exactly the Euclidean projection formula (20) for scalar R.

8.3 Exact nonlinear remainder and a certified safe invariant ellipsoid

Set $\xi_1 = x_1 - 2$, $\xi_2 = x_2$. The nonlinear sliding dynamics is exactly

$$\dot{\xi} = A\xi + Bu + r(\xi), \; r(\xi) = \begin{bmatrix} 0 \\ -3\xi_1^2 - \frac{1}{2}\xi_1^3 - 0.15\xi_1^2\xi_2 \end{bmatrix}. \tag{39}$$

For the unsaturated feedback $u = -K\xi$, let $V(\xi) = \xi^T P\xi$, $W = Q + K^T RK$. Using the CARE identity and (39), differentiation gives the exact relation

$$\dot{V} = -\xi^T W\xi + 2(P\xi)_2 r_2(\xi). \tag{40}$$

Indeed, $\dot{V} = \xi^T\big[(A - BK)^T P + P(A - BK)\big]\xi + 2\xi^T P r(\xi)$, and the CARE implies $(A - BK)^T P + P(A - BK) = -(Q + K^T RK) = -W$. Numerically, $\lambda_{\min}(P) = 1.44148$, $\lambda_{\max}(P) = 11.02651$, $\lambda_{\min}(W) = 5.59669$.

The exit surface is $\xi_1 = 1$. Minimizing V over this affine line gives

$$\rho_\Sigma = \min_{\xi_2 \in \mathbb{R}} \big(p_{11} + 2p_{12}\xi_2 + p_{22}\xi_2^2\big) = p_{11} - \frac{p_{12}^2}{p_{22}} \approx 10.60188.$$

For the actuator bound $|u| \le 3$, Cauchy–Schwarz in the P-metric gives $|K\xi|^2 = \big|(KP^{-1/2})(P^{1/2}\xi)\big|^2 \le (KP^{-1}K^T)V(\xi)$. Therefore the entire ellipsoid $V \le \rho_U$ is compatible with $|u| \le 3$ when $\rho_U = \frac{9}{KP^{-1}K^T} \approx 1.50079$.

It remains to establish nonlinear positive invariance. Put $a_1 = (P^{-1})_{11} = 0.0943229$, $a_2 = (P^{-1})_{22} = 0.690099$, $p_{22} = 1.499214$. and let $\gamma = \lambda_{\min}(W, P) = 0.971073$, the smallest generalized eigenvalue of $Wv = \gamma Pv$. The generalized eigenvalue inequality gives

$$\xi^T W\xi \ge \gamma\xi^T P\xi = \gamma V(\xi). \tag{41}$$

The coordinate functionals satisfy the exact Cauchy–Schwarz estimates

$$\xi_1^2 \le a_1 V,\ \xi_2^2 \le a_2 V,\ |(P\xi)_2|^2 \le p_{22} V. \tag{42}$$

Consequently, on $V(\xi) \le \rho$, $|\xi_1| \le \sqrt{a_1\rho}$, $|\xi_2| \le \sqrt{a_2\rho}$. Since $r_2(\xi) = -\xi_1^2\left(3 + \frac{1}{2}\xi_1 + 0.15\xi_2\right)$, we obtain the sharper bound retaining the factor V:

$$|r_2(\xi)| \le a_1 V\left(3 + \frac{1}{2}\sqrt{a_1\rho} + 0.15\sqrt{a_2\rho}\right). \tag{43}$$

Also, from (42), $|(P\xi)_2| \le \sqrt{p_{22}V} \le \sqrt{p_{22}\rho}$. Combining (40), (41), and (43) gives, for $0 < V \le \rho$,

$$\dot{V} \le -V\Big[\gamma - 2a_1\sqrt{p_{22}\rho}\Big(3 + \tfrac{1}{2}\sqrt{a_1\rho} + 0.15\sqrt{a_2\rho}\Big)\Big]. \tag{44}$$

The bracket is a strictly decreasing function of $\rho > 0$, is positive at $\rho = 0$, and we denote its unique positive root, the nonlinear-invariance threshold, by $\rho_{\mathrm{NL}} \approx 1.57569$, where the subscript "NL" denotes nonlinear invariance. Hence every ellipsoid $V \le \rho$ with $\rho < \rho_{\mathrm{NL}}$ is strictly invariant under the nonlinear unsaturated feedback.

The final certified Lyapunov level is

$$\rho_{\mathrm{safe}} = \min\{\rho_{\mathrm{NL}}, \rho_U, \rho_\Sigma\} = 1.50079. \tag{45}$$

At this level the bracket in (44) is still strictly positive:

$$\gamma - 2a_1\sqrt{p_{22}\rho_{\mathrm{safe}}}\Big(3 + \tfrac{1}{2}\sqrt{a_1\rho_{\mathrm{safe}}} + 0.15\sqrt{a_2\rho_{\mathrm{safe}}}\Big) \approx 0.02574. \tag{46}$$

Proposition 8.1 (Certified nonlinear safe ellipsoid)**.** *For the Duffing–Rayleigh closed loop* (39), (37)*, the set* $\Omega_{\mathrm{safe}} := \{\xi : \xi^T P\xi \le \rho_{\mathrm{safe}}\}$ *is positively invariant. Every trajectory starting in* Ω_{safe} *satisfies the actuator bound* $|u(t)| \le 3$*, remains strictly separated from the exit surface* $\xi_1 = 1$*, and obeys*

$$\dot{V} \le -0.02574\, V \tag{47}$$

for every nonzero state in Ω_{safe}*.*

Proof Because $\rho_{\mathrm{safe}} < \rho_{\mathrm{NL}}$, inequality (44) and the monotonicity of its bracket imply (47) throughout $0 < V \le \rho_{\mathrm{safe}}$. In particular, on the boundary $V = \rho_{\mathrm{safe}}$ the derivative points strictly inward, so the Lyapunov sublevel set is positively invariant.

Next, $\rho_{\mathrm{safe}} \le \rho_U$. Therefore, for every $\xi \in \Omega_{\mathrm{safe}}$, $|u|^2 = |K\xi|^2 \le (KP^{-1}K^T)V \le (KP^{-1}K^T)\rho_U = 9$, so $|u| \le 3$ everywhere in the invariant set. Hence the saturated implementation (38) coincides with the unsaturated LQR law throughout Ω_{safe}.

Finally, $\rho_{\mathrm{safe}} < \rho_\Sigma$, while ρ_Σ is the minimum of V on the exit line $\xi_1 = 1$. Thus no point of Ω_{safe} can lie on the exit surface. Since Ω_{safe} is invariant, a trajectory starting inside it cannot reach the exit surface at any later time. □

At $(x_1(0), x_2(0)) = (2.3, 0)$, $V(\xi_0) \approx 0.98719 < \rho_{\mathrm{safe}}$, so this initial condition belongs to the certified nonlinear invariant set.

8.4 High-order barrier condition

For $h = 3 - x_1$, the relative degree is two because $\dot{h} = -x_2$. For a margin $\delta \ge 0$, define $\psi_0 = 3 - \delta - x_1$, $\psi_1 = -x_2 + k_1(3 - \delta - x_1)$. The HOCBF inequality $\dot{\psi}_1 + k_2\psi_1 \ge 0$

gives $u \leq -4 + 0.5x_1^3 + D(x_1)x_2 - (k_1 + k_2)x_2 + k_1k_2(3 - \delta - x_1)$. It is an online safety condition only when the inequality and the actuator bounds are jointly feasible and the initial HOCBF conditions $\psi_0(0) \geq 0$, $\psi_1(0) \geq 0$ hold. In the constrained comparison below, $\delta = 1$, $k_1 = k_2 = 5$, and $(x_1(0), x_2(0)) = (1.9, 0.4)$, so $\psi_0(0) = 0.1$ and $\psi_1(0) = 0.1$; hence the initial high-order barrier conditions are satisfied.

The same relative-degree-two geometry also gives an exact control on a smooth active boundary arc. If $h = \delta$ and $\dot{h} = 0$, then $x_1 = 3 - \delta$, $x_2 = 0$. Tangency at the next derivative requires $\ddot{h} = -\dot{x}_2 = 0$, and therefore $u_b = -4 + \frac{1}{2}(3 - \delta)^3$. For the numerical safety core $\delta = 1$, this gives $u_b = 0$ at the boundary point $(x_1, x_2) = (2, 0)$. This closed-form condition is the higher-relative-degree analogue of Proposition 6.3.

8.5 Baseline suppression from the certified ellipsoid

From $(x_1(0), x_2(0)) = (2.3, 0)$, the uncontrolled selected on-manifold trajectory reaches $x_1 = 3$ at $t_{\text{exit}} \approx 10.74379$, whereas the LQR closed loop converges to $(2, 0)$ while remaining inside the certified set (45). Figures 1 and 2 show the phase trajectory and the feedback transient. For $T = 20$, the reproduced performance values are

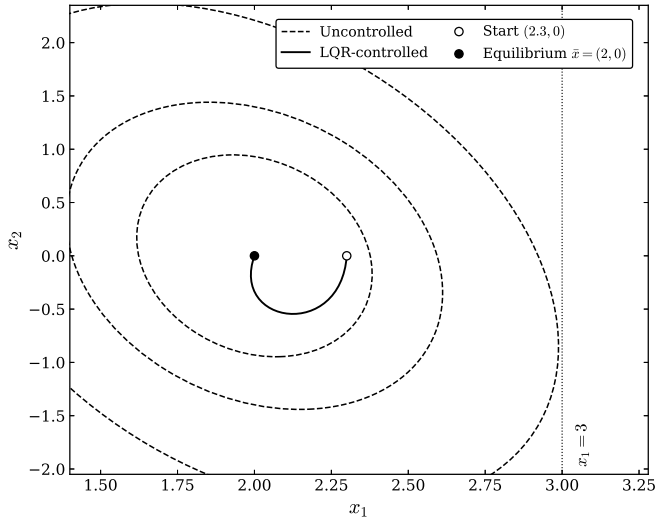


Fig. 1 Selected on-manifold trajectories from $(2.3, 0)$. The uncontrolled orbit reaches the exit boundary $x_1 = 3$, whereas the controlled trajectory remains in the sliding domain and converges to $(2, 0)$

8.6 Constrained nonlinear finite-horizon optimization

To investigate horizon-based constrained optimization with a path constraint, consider the more demanding initial state $(x_1(0), x_2(0)) = (1.9, 0.4)$ and the conservative safety core $h \geq 1$, equivalently $x_1 \leq 2$. Over $T = 8$, with the same tangential weight $Q = \text{diag}(10, 2)$ and control weight $R = 0.5$ as in the LQR design above, we solve

$$\min_u \frac{1}{2}\xi(T)^T Q_T \xi(T) + \frac{1}{2}\int_0^T (\xi^T Q \xi + 0.5u^2)\, dt, \tag{48}$$

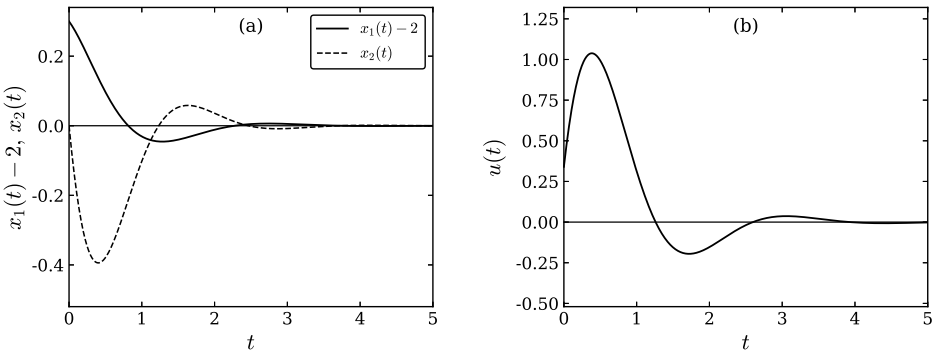


Fig. 2 Closed-loop transient under the LQR feedback over $0 \le t \le 5$. (a) State deviations $x_1(t) - 2$ and $x_2(t)$. (b) Control input $u(t) = -1.483315[x_1(t) - 2] - 2.998428x_2(t)$. Both the state deviations and the control input decay to zero

Table 1 Baseline nonlinear LQR performance.

Quantity	Value
Uncontrolled exit time t_{exit}	10.74379
Maximum controlled $x_1(t)$	2.30000
Minimum exit margin $3 - x_1(t)$	0.70000
Maximum control magnitude	1.23482
Control energy $\int_0^{20} u^2 dt$	0.89940
Settling time (permanent entry into $\|\xi\|_2 \le 10^{-2}$)	3.38609
Nonlinear quadratic cost	0.51849

$$\text{s.t. } (35),\ |u| \le 3,\ x_1(t) \le 2,$$

with $Q_T = \text{diag}(20, 5)$. A direct transcription with piecewise-constant controls and fourth-order Runge–Kutta integration was solved with the Sequential Least Squares Programming (SLSQP) algorithm, a sequential quadratic programming method. Because the nonlinear transcription is nonconvex, the resulting SLSQP point is interpreted as a numerically computed locally stationary candidate, not as a certificate of global optimality. To remove between-node violation under zero-order-hold validation, the transcription used the slightly tightened node bound $x_1 \le 1.9998$; the reported trajectory was then independently reintegrated on a fine time grid against the original bound $x_1 \le 2$.

The unconstrained LQR has the smallest quadratic cost but violates the prescribed safety core, reaching $x_1 = 2.04764$. The HOCBF-filtered LQR with $k_1 = k_2 = 5$ satisfies the constraint but incurs the largest control modification. The constrained nonlinear transcription satisfies the path constraint while reducing the evaluated horizon cost relative to the HOCBF filter. A mesh-refinement check gave the following first-order optimality diagnostics for the SLSQP transcription. The KKT residual is the infinity norm of the discrete Lagrangian stationarity residual, and the path residual is the maximum violation of the tightened node constraint $x_1 \le 1.9998$. For $N = 120$, the SLSQP solution has $\max|u| = 1.45994$ and exact zero-order-hold energy $\Delta t \sum_{i=0}^{119} u_i^2 = 0.57189$. Interval-by-interval high-accuracy reintegration, with

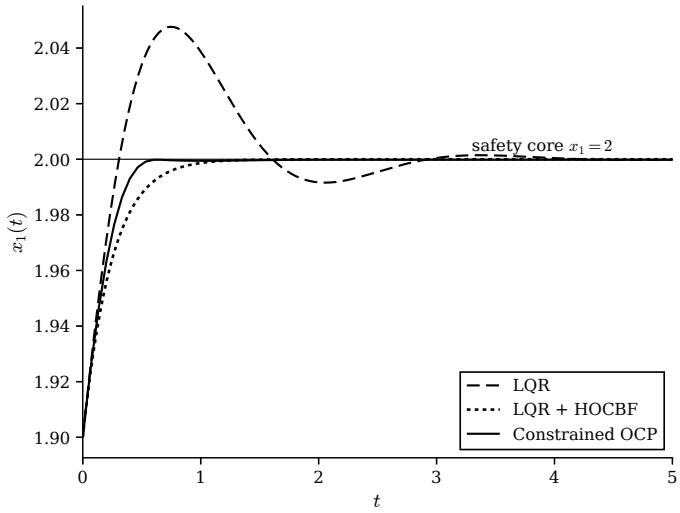


Fig. 3 Position response for the unconstrained LQR, the HOCBF-filtered LQR, and the constrained nonlinear finite-horizon OCP. The horizontal line is the imposed safety core $x_1 = 2$

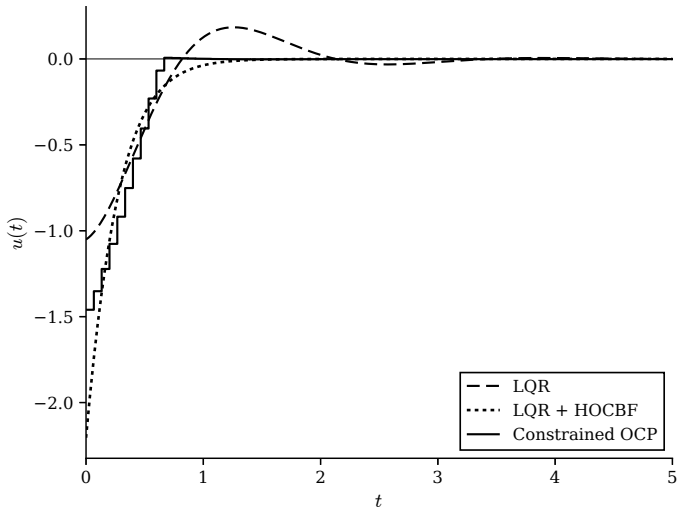


Fig. 4 Control histories for the constrained comparison. The HOCBF filter applies the strongest instantaneous correction, whereas the horizon OCP anticipates the path constraint and uses a less aggressive peak input

Table 2 Comparison for the constrained finite-horizon experiment. The OCP values correspond to the fine-grid validation of the $N = 120$ transcription.

Method	Cost	$\max x_1$	$\max \lvert u \rvert$	$\int u^2 dt$
LQR	0.14363	2.04764	1.05104	0.35387
LQR + HOCBF	0.19052	2.00000	2.20490	0.65569
Constrained nonlinear OCP	0.17369	1.99984	1.45994	0.57189

Table 3 Mesh refinement and discrete first-order residuals for the SLSQP transcription.

N	Objective	KKT residual	Max path residual	Iterations
40	0.17845070	6.76×10^{-6}	4.8×10^{-13}	20
80	0.17457162	1.63×10^{-6}	5.4×10^{-13}	26
120	0.17392566	2.22×10^{-6}	5.6×10^{-14}	30

the control discontinuities treated exactly at the mesh boundaries, gives $\max x_1 = 1.99983709$, $J_{\text{fine}} = 0.17368648$, so the original continuous path bound $x_1 \leq 2$ is satisfied. The difference between J_{120} and J_{fine} is due to transcription and quadrature discretization.

As an independent nonlinear-programming cross-check, the same $N = 120$ transcription was implemented in CasADi and solved with the Interior Point OPTimizer (IPOPT). Five substantially different initial guesses—LQR, HOCBF-filtered LQR, zero control, half-scaled LQR, and a smooth random bounded input—all converged to the same objective to the displayed precision: $J_{\text{IPOPT}} = 0.1739256581$, within 5×10^{-10} of the SLSQP objective. The runs required 19–24 IPOPT iterations; the final primal infeasibility was at most 1.1×10^{-12} and the final dual infeasibility at most 7.3×10^{-12}. The resulting peak input was 1.45995. This solver and initialization agreement is evidence for a stable local discretized solution, but it is not used as a claim of global optimality. The analytical safety guarantee remains Proposition 8.1.

8.7 Full regularized dynamics and convergence to the selected on-manifold problem

The exact selected on-manifold dynamics does not require $\epsilon \to 0$. For nearby off-manifold initial data, Theorem 3.2 predicts exponential normal collapse on the $O(\epsilon^2)$ time scale and a generic tangential deviation of order $O(\epsilon^3)$ when the initial normal offset is $O(\epsilon)$. Because the simulations use state feedback, Corollary 3.3 applies directly to the LQR closed loop. The present Duffing example is more favorable because its tangential dependence on $y - y^*$ begins quadratically. We therefore integrate the full regularized three-dimensional system with the LQR law for $\epsilon \in \{0.20, 0.10, 0.05, 0.025\}$, $y(0) = 3 \pm \epsilon$, and compare its tangential state with the selected closed-loop solution. Define $E_x(\epsilon) = \max_{t \in [0.25,5]} \|x_\epsilon(t) - x_s(t)\|_2$.

The worst error over the two signs of the initial normal offset is reported in Table 4. Here, the normal e-fold time is defined as the first output-grid time (grid spacing 10^{-3}) at which $|y(t) - y^*| \leq e^{-1}|y(0) - y^*|$. Its resolution accounts for the rounding of the

two smallest entries. A log–log fit of these four tangential errors gives an empirical

Table 4 Off-manifold convergence of the full regularized controlled system.

ϵ	$\max E_x(\epsilon)$	Normal e-fold time
0.200	5.04×10^{-4}	0.101
0.100	2.36×10^{-5}	0.023
0.050	1.34×10^{-6}	0.006
0.025	8.07×10^{-8}	0.002

slope of approximately 4.20. This high order is specific to the example because the tangential forcing $\psi(y) = 4 - 0.5(y-3)^2$ has no linear dependence on the normal displacement at $y = 3$; it is not claimed as a general convergence order.

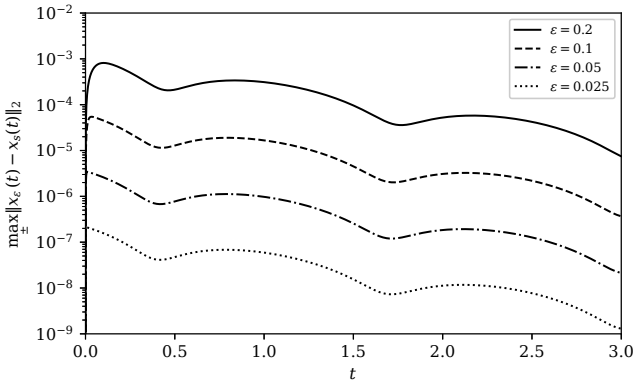


Fig. 5 Tangential error between the full regularized and selected on-manifold controlled trajectories for off-manifold initial data $y(0) = 3 \pm \epsilon$

8.8 Sensitivity of normal attraction

For the Duffing family with $\varphi(y) = -2r(y-3)$ and $g = \beta(y - x_1)$, the on-manifold normal rate is $\lambda_\perp = -\frac{2r\,\beta(3-x_1)}{\epsilon^2}$. Thus uncertainty in r or β changes the contraction rate multiplicatively but does not change the selected tangential dynamics as long as $r > 0$, $\beta > 0$, and the singular hyperplane is fixed. At $x_1 = 2.3$, $\epsilon = 0.1$, the baseline magnitude is 70; allowing independent $\pm 10\%$ variations in r and β gives the interval $[56.7, 84.7]$. The attraction therefore remains strong throughout this uncertainty box.

A more consequential perturbation is an error in the location of the singular zero. The following calculation quantifies one structured version of this mismatch rather than claiming general robust invariance. Let the actual singular coefficient be

$$\varphi_\Delta(y) = -2r\big(y - (y^* + \Delta)\big), \tag{49}$$

while the calibrated tangential constitutive function $\psi(y) = R_0 - r(y - y^*)^2$, the function $g = \beta(y - x_1)$, and the nominal feedback (37) are kept unchanged. The true selected hyperplane is then $y = y^* + \Delta$, and its tangential dynamics differs from (35)

by the constant input disturbance

$$d_\Delta = -\alpha r \Delta^2 = -\frac{1}{2}\Delta^2 \tag{50}$$

in the second state equation.

Proposition 8.2 (Structured robustness to localization error)**.** *Under the mismatch model* (49)*, the same nominal ellipsoid* Ω_{safe} *of Proposition 8.1 remains positively invariant and actuator-compatible whenever* $|\Delta| < 0.16047$*. For every such* Δ*,* Ω_{safe} *is also strictly separated from the shifted exit surface* $x_1 = 3 + \Delta$*.*

Proof Let $b_{\text{safe}} = 0.0257387$ denote the positive bracket in (46). On the boundary $V = \rho_{\text{safe}}$, the added disturbance (50) modifies the Lyapunov derivative by $2(P\xi)_2 d_\Delta$. Therefore (42) gives $\dot{V} \le -\rho_{\text{safe}} b_{\text{safe}} + 2\sqrt{p_{22}\rho_{\text{safe}}}\,|d_\Delta|$. The right-hand side is strictly negative provided $|d_\Delta| < \frac{\sqrt{\rho_{\text{safe}}}\, b_{\text{safe}}}{2\sqrt{p_{22}}} \approx 0.0128761$. Since $|d_\Delta| = \frac{1}{2}\Delta^2$, this condition is exactly $|\Delta| < 0.16047$ to the displayed precision. The actuator estimate is unchanged because it depends only on K, P, and ρ_{safe}. The shifted exit line is $\xi_1 = 1 + \Delta$; its minimum Lyapunov level is $(1+\Delta)^2\rho_\Sigma$. Even at the worst endpoint $\Delta = -0.16047$, this level exceeds 7.47, which is far above $\rho_{\text{safe}} = 1.50079$. Hence the invariant ellipsoid cannot intersect the shifted exit surface. □

This proposition addresses only the explicitly defined localization-error model (49); simultaneous uncertainty in g, ψ, the controller, or the geometry requires a broader robust-control formulation.

9 Additional analytical and numerical examples

The previous example is nonlinear and local. To test different parts of the theory, we now consider four further systems: an exactly solvable finite-horizon transfer, a higher-dimensional multi-input stabilization problem, periodic tracking with a two-sided exit constraint, and a dimensionless turbomachinery-motivated surrogate of cavitating-pump surging.

9.1 Exact minimum-energy transfer inside the sliding domain

Consider the implicitly singularly perturbed system

$$\begin{cases} \dot{x}_1 = x_2, \\ \dot{x}_2 = u, \qquad\qquad \beta > 0. \\ -(y-1)\dot{y} = \beta(y - x_1), \end{cases} \tag{51}$$

Here $y^* = 1$, $\varphi'(1) = -1$, and on the singular hyperplane $h(x) = \beta(1 - x_1)$, $\mathcal{D} = \{x_1 < 1\}$. The regularization-selected on-manifold dynamics is the double integrator. For fixed $T > 0$ and $0 < d < 1$, consider

$$\min_u \; J(u) = \frac{1}{2}\int_0^T u(t)^2 dt, \; x(0) = (0,0), \; x(T) = (d,0). \tag{52}$$

Proposition 9.1 (Closed-form exit-safe minimum-energy transfer)**.** *The unique optimizer of* (52) *is*

$$u^*(t) = \frac{6d}{T^2}\left(1 - 2\frac{t}{T}\right). \tag{53}$$

The corresponding state is

$$x_1^*(t) = d\left[3\left(\frac{t}{T}\right)^2 - 2\left(\frac{t}{T}\right)^3\right], \tag{54}$$

$$x_2^*(t) = \frac{6d}{T}\left(\frac{t}{T} - \left(\frac{t}{T}\right)^2\right), \tag{55}$$

and the optimal cost is $J^* = \frac{6d^2}{T^3}$*. Moreover,* $0 \le x_1^*(t) \le d < 1$*, hence* $h(x^*(t)) \ge \beta(1-d) > 0$ *for the entire transfer. Thus the minimum-energy solution is analytically certified to avoid the singular exit.*

Proof For the selected double-integrator dynamics, take the Hamiltonian $H = \frac{1}{2}u^2 + p_1x_2 + p_2u$. The adjoint equations are $\dot{p}_1 = -\frac{\partial H}{\partial x_1} = 0$, $\dot{p}_2 = -\frac{\partial H}{\partial x_2} = -p_1$. Hence $p_1 = c_1$ is constant and $p_2(t) = -c_1t + c_2$ is affine. The Hamiltonian is strictly convex in u, and stationarity gives the unique pointwise minimizer $u^*(t) = -p_2(t) = c_1t - c_2$. Write this affine control as $u(t) = at + b$. Integration with $x_2(0) = 0$ gives $x_2(t) = \frac{1}{2}at^2 + bt$, and a second integration with $x_1(0) = 0$ gives $x_1(t) = \frac{1}{6}at^3 + \frac{1}{2}bt^2$. The terminal velocity condition $x_2(T) = 0$ yields $\frac{1}{2}aT^2 + bT = 0$, $b = -\frac{1}{2}aT$. Substitution into $x_1(T) = d$ gives $d = \frac{1}{6}aT^3 - \frac{1}{4}aT^3 = -\frac{1}{12}aT^3$, so $a = -\frac{12d}{T^3}$, $b = \frac{6d}{T^2}$. Therefore $u^*(t) = \frac{6d}{T^2}\left(1 - 2\frac{t}{T}\right)$, which proves (53). Substituting a and b into the integrated state formulas gives (54)–(55).

The objective is strictly convex in u on the affine space of controls satisfying the linear endpoint constraints. Hence the feasible stationary control just derived is the unique global minimizer. Its cost is

$$J^* = \frac{1}{2}\int_0^T \frac{36d^2}{T^4}\left(1 - 2\frac{t}{T}\right)^2 dt = \frac{18d^2}{T^3}\int_0^1 (1-2\tau)^2 d\tau = \frac{6d^2}{T^3}.$$

Finally, $\frac{d}{d\tau}(3\tau^2 - 2\tau^3) = 6\tau(1-\tau) \ge 0$ $(0 \le \tau \le 1)$, so the cubic shape function increases monotonically from 0 to 1. Thus $0 \le x_1^*(t) \le d < 1$, and consequently $h(x^*(t)) = \beta(1 - x_1^*(t)) \ge \beta(1-d) > 0$. The singular exit is therefore avoided for the entire optimal transfer. □

For $T = 2$, $d = 0.8$, and $\beta = 1$, one has $J^* = 0.48$, $\max|u^*| = 1.2$, and the minimum exit margin is $1 - d = 0.2$. Figures 6–7 show the exact optimal trajectory and input.

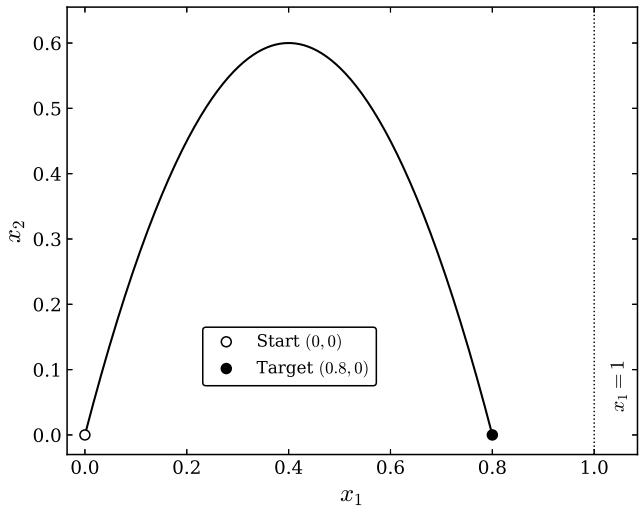


Fig. 6 Exact minimum-energy transfer for $T = 2$, $d = 0.8$. The cubic state trajectory terminates at $(0.8, 0)$ and remains strictly separated from the exit boundary $x_1 = 1$

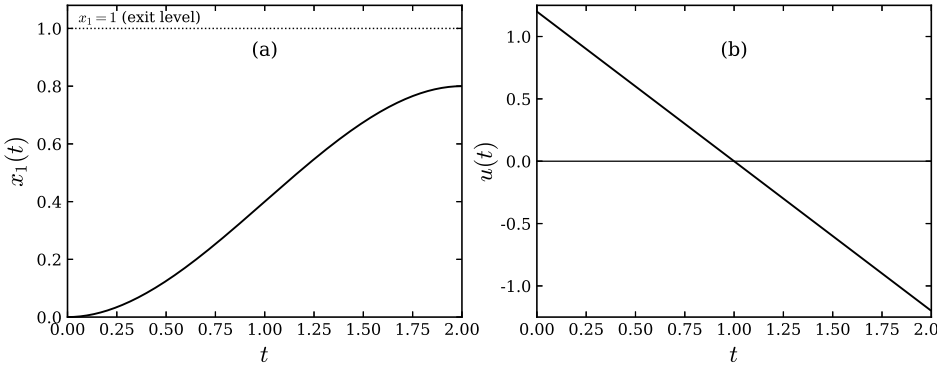


Fig. 7 Position and optimal control for the analytically solvable transfer. The control is affine in time and the state remains below the singular exit level for the entire horizon

9.2 Higher-dimensional two-mode system with two controls

To demonstrate that the construction is not tied to a two-dimensional sliding dynamics, let $\boldsymbol{x} = (q_1, v_1, q_2, v_2)^T$ and consider

$$\begin{cases} \dot{q}_1 = v_1, \\ \dot{v}_1 = 1.2q_1 - 0.1v_1 + 0.4q_2 + u_1, \\ \dot{q}_2 = v_2, \\ \dot{v}_2 = 0.3q_1 - 1.5q_2 - 0.2v_2 + 0.4u_1 + u_2, \\ -(y - 1.2)\dot{y} = \beta \left(y - q_1 - \dfrac{1}{2} q_2 \right), \end{cases} \qquad \beta = 1. \tag{56}$$

On $S = \{y = 1.2\}$, $h(\boldsymbol{x}) = 1.2 - q_1 - \frac{1}{2}q_2$, $\mathcal{D} = \{q_1 + 0.5q_2 < 1.2\}$. The selected on-manifold system has matrices

$$A = \begin{bmatrix} 0 & 1 & 0 & 0 \\ 1.2 & -0.1 & 0.4 & 0 \\ 0 & 0 & 0 & 1 \\ 0.3 & 0 & -1.5 & -0.2 \end{bmatrix}, \; B = \begin{bmatrix} 0 & 0 \\ 1 & 0 \\ 0 & 0 \\ 0.4 & 1 \end{bmatrix}. \tag{57}$$

The open-loop eigenvalues are approximately 1.06563, -1.16720, $-0.09921 \pm 1.23847i$, so the origin contains a genuinely unstable mode. With $Q = \mathrm{diag}(20, 2, 12, 2)$, $R = 3I_2$, the CARE gives

$$K \approx \begin{bmatrix} 4.04894 & 2.88416 & 0.81038 & 0.22850 \\ -0.33028 & -0.32768 & 0.93754 & 1.39045 \end{bmatrix}.$$

The closed-loop eigenvalues are $-1.51478 \pm 0.82448i$, $-0.81822 \pm 1.35620i$. Hence both modal pairs are exponentially stable.

Starting from $\boldsymbol{x}_0 = (0.6, 0, 0.4, 0)^T$, the initial safety margin is $h(\boldsymbol{x}_0) = 0.4$. The uncontrolled trajectory reaches the exit hyperplane at $t_{\mathrm{exit}} \approx 1.02096$, whereas the two-input LQR trajectory satisfies $\min_{t \in [0,8]} h(\boldsymbol{x}(t)) = 0.4$ and converges to the origin. The maximum control magnitudes are approximately 2.754 and 0.398, respectively. Figures 8–9 display the safety margin and the controlled modal response. For the

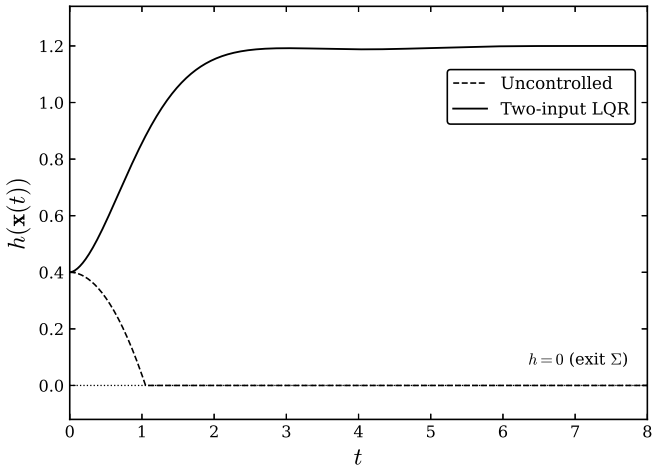


Fig. 8 Exit function for the four-dimensional sliding dynamics. The uncontrolled unstable mode drives h to zero in finite time, while the two-input optimal feedback keeps the trajectory strictly inside the sliding domain

minimum-energy and two-mode examples, an ϵ-sweep of the tangential error would be degenerate rather than informative: their tangential differential equations contain no y-dependence. With identical tangential initial data and the same admissible control, uniqueness therefore gives $\boldsymbol{x}_\epsilon(t) \equiv \boldsymbol{x}_s(t)$ for every $\epsilon > 0$, even when the normal coordinate starts off the selected hyperplane. The tracking example below contains the coupling term κy and is consequently used for a nontrivial cross-example regularization sweep.

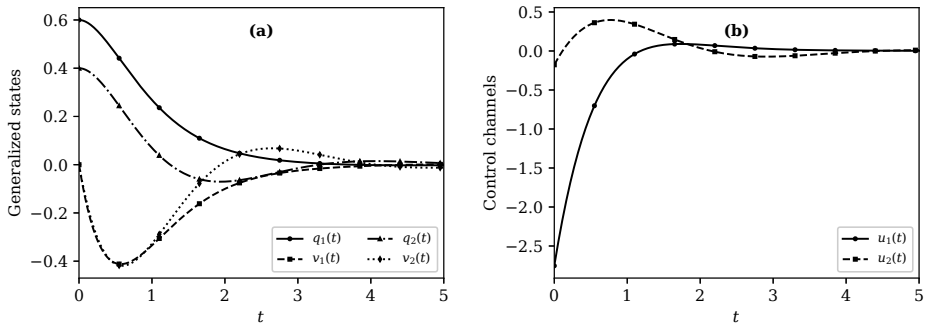


Fig. 9 Controlled two-mode transient. Both generalized coordinates and both optimal control channels decay to zero, illustrating the higher-dimensional and multi-input character of the framework

9.3 Periodic linear-quadratic (LQ) tracking with a certified two-sided exit margin

Consider a damped oscillator coupled to a singular variable,

$$\begin{cases} \dot{q} = v, \\ \dot{v} = -\omega_0^2 q - 2\zeta\omega_0 v + \kappa y + u, \\ -y\dot{y} = \beta\left[1 - \left(\dfrac{q}{q_e}\right)^2 - \eta y\right]. \end{cases} \tag{58}$$

Here $y^* = 0$, and on the sliding hyperplane $h(q) = \beta\left[1 - \left(\frac{q}{q_e}\right)^2\right]$, $\mathcal{D} = \{|q| < q_e\}$. Let the prescribed orbit be $q_r(t) = A_r \sin\Omega t$, $v_r(t) = A_r\Omega\cos\Omega t$, $A_r < q_e$. The exact feedforward input that generates the reference on S is $u_{ff} = \ddot{q}_r + 2\zeta\omega_0\dot{q}_r + \omega_0^2 q_r$. Write $e = (q - q_r, v - v_r)^T$ and $v_c = u - u_{ff}$. Then

$$\dot{e} = A_t e + B_t v_c,\ A_t = \begin{bmatrix} 0 & 1 \\ -\omega_0^2 & -2\zeta\omega_0 \end{bmatrix},\ B_t = \begin{bmatrix} 0 \\ 1 \end{bmatrix}. \tag{59}$$

Thus minimizing $J_c = \frac{1}{2}\int_0^\infty \left(e^T Q_t e + R_t v_c^2\right) dt$ produces an exact LQ tracker for the correction effort: $u = u_{ff} - K_t e$. For

$$\omega_0 = 1.2,\ \zeta = 0.12,\ \kappa = 0.4,\ \beta = 1,\ \eta = 0.3,\ Q_t = \mathrm{diag}(20, 4),\ R_t = 0.8. \tag{60}$$

we obtain

$$K_t \approx \begin{bmatrix} 3.76323 & 3.26297 \end{bmatrix},\ \lambda(A_t - B_t K_t) \approx -1.77549 \pm 1.43209i. \tag{61}$$

The parameters κ, β, η do not enter the on-manifold LQ metrics because $y \equiv 0$ on S; they are specified in (60) so that the complete three-dimensional regularized dynamics is reproducible off the manifold. Take $A_r = 0.8$, $\Omega = 0.7$, $q_e = 1.4$, and $(q(0), v(0)) = (0.25, -0.1)$. The tracking error becomes smaller than 7×10^{-5} by $t = 5$, the maximum correction magnitude is approximately 1.213, and $\min_{t\in[0,25]}(q_e - |q(t)|) \approx 0.6000$. Hence the unconstrained LQ tracking law, when evaluated on this example, remains a posteriori separated from the singular exit set by a substantial two-sided margin; the exit inequality is verified rather than imposed in the LQ optimization itself. Figures 10–11 show the resulting orbit tracking and the decomposition of the control input.

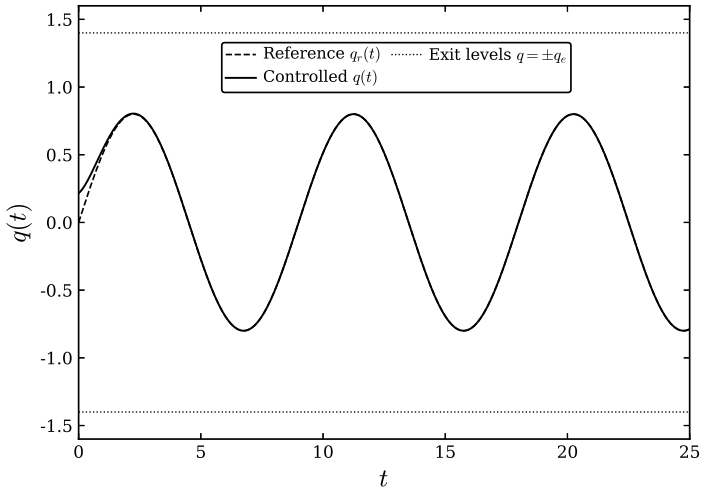


Fig. 10 Optimal tracking of the prescribed periodic position. After a short transient the controlled trajectory is visually indistinguishable from the reference and remains far from both exit levels $q = \pm q_e$

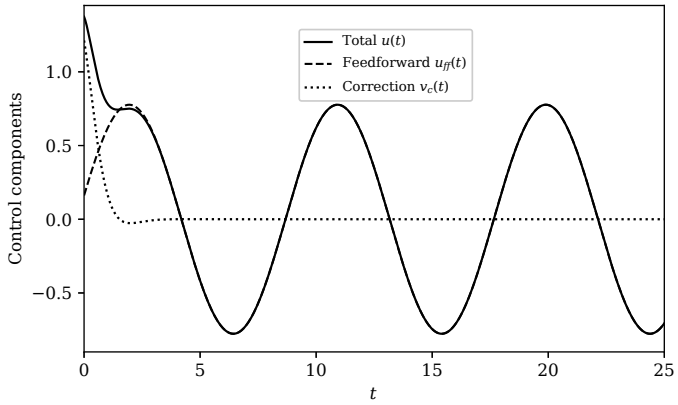


Fig. 11 Total control u, exact feedforward term u_{ff}, and optimal correction v_c. The correction decays rapidly, leaving only the periodic feedforward action needed to sustain the target orbit; the vertical range includes the initial correction peak

9.3.1 Off-manifold regularization sweep

To test the generic estimate of Theorem 3.2 in a second example with a genuinely nonzero tangential–normal coupling, we integrate the full regularized tracking model with $R_\epsilon(y) = -y/(y^2 + \epsilon^2)$, the feedback above, and $y(0) = \pm\epsilon$. Define $E_{\mathrm{tr}}(\epsilon) = \max_{t\in[0.25,5]} \|(q_\epsilon(t), v_\epsilon(t)) - (q_s(t), v_s(t))\|_2$, and report the larger value over the two signs of the initial normal offset. For $\epsilon = 0.20, 0.10, 0.05, 0.025$, the worst tangential errors $E_{\mathrm{tr}}(\epsilon)$ are 2.0354×10^{-3}, 2.1207×10^{-4}, 2.5228×10^{-5}, and 3.1085×10^{-6}, respectively. A least-squares fit in log–log coordinates gives slope 3.11, in agreement with the generic $O(\epsilon^3)$ tangential estimate for an $O(\epsilon)$ normal offset. In contrast, the

Duffing–Rayleigh example has the higher empirical slope 4.20 because its tangential dependence on $y - y^*$ begins quadratically.

9.4 Turbomachinery-motivated reduced surrogate of cavitating-pump surging

Cavitating centrifugal pumps provide a concrete application context in which self-excited surging and its damping have been observed and modeled [3]. To demonstrate how the present regular-channel construction enters such a setting without claiming parameter identification from those experiments, consider the dimensionless local surrogate

$$\begin{cases} \dot{q} = \sigma(q - \bar{q}) - \chi(q - \bar{q})^3 + \kappa_p(y - y^*) + u, \\ -(y - y^*)\dot{y} = \beta(y - q). \end{cases} \tag{62}$$

where q is a nondimensional flow-coordinate deviation and y is a cavitation/pressure-like internal coordinate. We set $\bar{q} = 1$, $y^* = 1.6$, $\sigma = \chi = \beta = 1$, $\kappa_p = 0.25$. The singular hyperplane is $S = \{y = 1.6\}$, its attracting domain is $q < 1.6$, and the selected dynamics is $\dot{z} = z - z^3 + u$, $z = q - 1$. Thus the regular-channel input changes the flow dynamics but does not move either S or its exit $q = 1.6$. From $q(0) = 1.2$, the uncontrolled selected trajectory reaches the exit at $t_{\text{exit}} = 1.30134$. With the simple stabilizing regular-channel law $u = -2.5z$, the selected closed loop is $\dot{z} = -1.5z - z^3$. Over $0 \le t \le 8$, it has minimum exit margin $1.6 - q(t) = 0.40000$, peak control $\max|u| = 0.50000$, and control energy $\int_0^8 u^2 dt = 0.08224$, while $q(8) = 1.000001$. This example is deliberately a reduced, dimensionless surrogate: it illustrates the geometry-preserving control mechanism in a turbomachinery setting motivated by [3], but it is not presented as a fit or validation against those experimental data.

10 Numerical reproducibility and scope of the event-free theory

All numerical ODE results use adaptive Runge–Kutta integration with relative tolerance at most 10^{-9} and absolute tolerance at most 10^{-11}; discontinuous zero-order-hold controls are revalidated interval by interval so that solver steps do not cross control jumps unnoticed. CARE matrices were obtained from a standard continuous-time Riccati solver. The constrained OCP uses zero-order-hold controls, fourth-order Runge–Kutta state propagation inside the transcription, $|u| \le 3$, and the tightened node constraint $x_1 \le 1.9998$. The SLSQP implementation uses analytical first derivatives of the discrete objective and path constraints for the residual check. The same transcription was independently reconstructed in CasADi and solved with IPOPT from five initial guesses. Because the nonlinear program is nonconvex, neither solver certifies global optimality or uniqueness; the reported solution is a numerically stable locally stationary candidate. Table 3, the independent IPOPT solve, and fine reintegration provide complementary checks of stationarity, constraint satisfaction, mesh stabilization, and implementation consistency.

The present optimality theory is intentionally event-free: the controller is designed to remain in the attracting sliding region and to make ejection inaccessible. We do not

claim to optimize a complete relaxation cycle containing exit, fast excursion, and reentry. Such a problem would require event-sensitive transversality and costate jumps, as well as a hybrid multiple-shooting or transcription framework. For a smooth event surface $s(z) = 0$, a typical adjoint relation has the form $\lambda^+ = \lambda^- + \nu \nabla s(z_e)$, with ν fixed by event-time transversality and Hamiltonian matching. Developing that event-crossing theory for the present unbounded implicit system is left for future work rather than being folded into the current claims.

11 Discussion and conclusions

The framework separates four notions that are often conflated in singular-control applications. First, the constrained nonlinear transcription provides a numerically computed locally stationary approximation to the finite-horizon path-constrained problem. Second, PMP and HJB characterize smooth optimality on the regularization-selected invariant dynamics, and the tangential optimality system is exact for every $\epsilon > 0$. Third, LQR is optimal only for the local linear-quadratic approximation. Fourth, a CBF/HOCBF filter supplies forward-invariance protection by minimizing an instantaneous modification of a nominal command; when active, it is not generally the horizon optimizer.

The exact invariance of the reciprocal regularization is the central structural simplification. It avoids an unsupported application of the classical Filippov construction to the unbounded field g/φ, and it avoids treating $y = y^*$ as a classical solution of the original implicit equation where $g(\boldsymbol{x}, y^*) \neq 0$. Instead, the regularization selects a generalized invariant dynamics on the loss-of-rank hypersurface. This viewpoint also clarifies the distinction from both classical singular-perturbation control and standard DAE optimal control. Classical singular-perturbation control starts from an explicit small parameter and a pre-existing slow–fast decomposition [8]; regular DAE theory addresses consistency and optimality for descriptor systems under regularity/index assumptions [9–12]. Here, by contrast, the time-scale separation is generated by approach to a state-dependent rank-loss hypersurface, and accessibility of that hypersurface is itself part of the controlled geometry. Relative to the piecewise-smooth regularization strategy of Westenbroek et al. [16], the distinctive tradeoff is now explicit: the present method is less general with respect to nonsmooth switching structure, but gains exact finite-ϵ invariance of the prescribed rank-loss hypersurface and therefore exact on-manifold optimal-control equivalence. The exact on-manifold adjoint reduction then follows because the potentially problematic normal multiplier term is multiplied by $R_\epsilon(y^*) = 0$.

The nonlinear safety calculation is equally important. Geometric separation from the exit surface and compatibility with actuator bounds do not by themselves prove positive invariance. In the Duffing–Rayleigh example, inequality (44) supplies the missing nonlinear estimate and yields $\rho_{\mathrm{NL}} > \rho_U$, so the entire actuator-compatible Riccati ellipsoid is rigorously invariant. Proposition 8.2 further shows, for a precisely defined localization-error model, that the same ellipsoid survives a zero-location mismatch of magnitude up to approximately 0.160. The state-constrained OCP then addresses a different question: how to distribute control effort over a finite horizon

when a prescribed safety core must be respected. The pump-surging surrogate in Section 9.4 provides a separate engineering interpretation of regular-channel actuation while deliberately avoiding any claim of experimental parameter identification.

Several limitations remain. Exact equality of the two optimal-control problems applies only to initial states, references, and terminal targets on the selected invariant hyperplane. For nearby initial states, Theorem 5.4 gives uniform convergence of costs on a common safety-core control class, while Corollary 5.5 gives uniform optimal-value convergence for starting times bounded a fixed positive distance away from the terminal time. No off-manifold convergence theorem for costates is claimed. Optimizer convergence is obtained only under the additional compactness, lower-semicontinuity, and uniqueness assumptions of Proposition 5.6. The localization calculation of Proposition 8.2 covers only one structured mismatch model; general simultaneous uncertainty in the zero location, the vector fields, and the constraints, together with event-crossing optimal control, stochastic disturbances, and robust state constraints, remains a natural extension.

A geometry-preserving optimal-control framework has been established for implicitly singularly perturbed systems with a state-dependent loss-of-rank hypersurface. Regular-channel actuation leaves this geometry fixed, while the reciprocal Cauchy regularization selects an exact invariant generalized dynamics on the hypersurface for every $\epsilon > 0$ and makes it normally attracting in the sliding domain. For on-manifold control problems, the regularized and selected lower-dimensional problems have identical state maps, costs, minimizers, tangential Pontryagin systems, and restricted value functions without taking a singular limit; the same exact equivalence persists when identical tangential path constraints, including the exit margin, are imposed. For $O(\epsilon)$ off-manifold initial offsets, the costs differ by only $O(\epsilon^3)$ on a fixed horizon; the same order holds for safety-core optimal values uniformly for starting times bounded away from the terminal time.

Exit avoidance has been formulated as a genuine state-constrained OCP, with explicit boundary-arc geometry and a separate CBF/HOCBF safety layer. Local CARE/LQR design supplies a stabilizing baseline, while an explicit nonlinear Lyapunov estimate converts the Riccati metric into a certified invariant safe set. For the Duffing–Rayleigh system, $\rho_{\mathrm{NL}} = 1.57569$, $\rho_U = 1.50079$, and $\rho_\Sigma = 10.60188$, giving the certified invariant-ellipsoid level $\rho_{\mathrm{safe}} = 1.50079$. A constrained nonlinear direct-transcription experiment demonstrates the distinction between unconstrained LQR, HOCBF filtering, and a locally stationary horizon-based optimization candidate. Full regularized simulations confirm rapid collapse of nearby trajectories toward the exact selected on-manifold dynamics; an independent tracking sweep gives the generic cubic scaling with empirical slope 3.11, while two decoupled examples exhibit exact tangential coincidence for every ϵ. A structured zero-localization calculation gives a quantitative robustness radius for the certified ellipsoid, and a dimensionless cavitating-pump surrogate demonstrates how regular-channel actuation can be interpreted in a concrete turbomachinery setting without moving the singular geometry. These results provide a stronger optimal-control interpretation of the singular geometry than a purely formal sliding or LQR argument.

Data availability. No external datasets were used. Numerical results, including the localization-error calculation, the additional off-manifold tracking sweep, and the pump-surging surrogate, are reproducible from the equations, parameters, and control weights reported in the manuscript.

Code availability. A supplementary script reproducing the principal ODE/CARE calculations, the zero-order-hold/fourth-order Runge–Kutta constrained transcription, the SLSQP first-order residual checks, the independent CasADi/IPOPT cross-check, and the additional examples of Section 9 is available from the corresponding author on request.

References

[1] Cardin PT, da Silva PR, Teixeira MA (2012) Implicit differential equations with impasse singularities and singular perturbation problems. *Isr J Math* 189:307–322. https://doi.org/10.1007/s11856-011-0169-3.

[2] Sotomayor J, Zhitomirskii M (2001) Impasse singularities of differential systems of the form $A(x)x' = F(x)$. *J Differential Equations* 169:567–587. https://doi.org/10.1006/jdeq.2000.3908.

[3] Gotsulenko VV, Gotsulenko VN (2013) Self-oscillations (surging) of a single-stage centrifugal pump in the cavitation regime and their damping. *J Eng Phys Thermophys* 86:913–920. https://doi.org/10.1007/s10891-013-0911-2.

[4] Gotsulenko VV (2014) Self-oscillations in implicit singularly perturbed dynamical systems on the plane. *Russ J Nonlinear Dyn* 10:157–176. https://doi.org/10.20537/nd1402003.

[5] Filippov AF (1988) *Differential Equations with Discontinuous Righthand Sides*. Kluwer, Dordrecht.

[6] Utkin VI (1992) *Sliding Modes in Control and Optimization*. Springer, Berlin.

[7] di Bernardo M, Budd CJ, Champneys AR, Kowalczyk P (2008) *Piecewise-smooth Dynamical Systems: Theory and Applications*. Springer, London.

[8] Kokotović PV, Khalil HK, O'Reilly J (1999) *Singular Perturbation Methods in Control: Analysis and Design*. SIAM, Philadelphia. https://doi.org/10.1137/1.9781611971118.

[9] Gerdts M (2015) A survey on optimal control problems with differential-algebraic equations. In: *Surveys in Differential-Algebraic Equations II*, Differential-Algebraic Equations Forum. Springer, Cham, pp 103–161. https://doi.org/10.1007/978-3-319-11050-9_3.

[10] Roubíček T, Valášek M (2002) Optimal control of causal differential-algebraic systems. *J Math Anal Appl* 269:616–641. https://doi.org/10.1016/S0022-247X(02)00040-9.

[11] Kunkel P, Mehrmann V (2008) Optimal control for unstructured nonlinear differential-algebraic equations of arbitrary index. *Math Control Signals Syst* 20:227–269. https://doi.org/10.1007/s00498-008-0032-1.

[12] Ilchmann A, Leben L, Witschel J, Worthmann K (2019) Optimal control of differential-algebraic equations from an ordinary differential equation perspective. *Optim Control Appl Methods* 40:351–366. https://doi.org/10.1002/oca.2481.

[13] Devdariani EN, Ledyaev YS (1999) Maximum principle for implicit control systems. *Appl Math Optim* 40:79–103. https://doi.org/10.1007/s002459900117.

[14] de Pinho MR (2016) On necessary conditions for implicit control systems. *Pure Appl Funct Anal* 1:185–206.

[15] Li A, Ye JJ (2018) Necessary optimality conditions for implicit control systems with applications to control of differential algebraic equations. *Set-Valued Var Anal* 26:179–203. https://doi.org/10.1007/s11228-017-0444-5.

[16] Westenbroek T, Xiong X, Ames AD, Sastry SS (2019) Optimal control of piecewise-smooth control systems via singular perturbations. In: *2019 IEEE 58th Conference on Decision and Control*, pp 3046–3053. https://doi.org/10.1109/CDC40024.2019.9029232.

[17] Kostyukova O, Kostina EA (2019) Necessary conditions for optimality in problems of optimal control of systems with discontinuous right-hand side. *Differ Equ* 55:374–389. https://doi.org/10.1134/S001226611903011X.

[18] Vinter RB (2000) *Optimal Control*. Birkhäuser, Boston.

[19] Vinter RB, Zheng H (1998) Necessary conditions for optimal control problems with state constraints. *Trans Am Math Soc* 350:1181–1204. https://doi.org/10.1090/S0002-9947-98-02129-1.

[20] Boccia A, de Pinho MDR, Vinter RB (2016) Optimal control problems with mixed and pure state constraints. *SIAM J Control Optim* 54:3061–3083. https://doi.org/10.1137/15M1041845.

[21] Pontryagin LS, Boltyanskii VG, Gamkrelidze RV, Mishchenko EF (1962) *The Mathematical Theory of Optimal Processes*. Interscience, New York.

[22] Cesari L (1983) *Optimization—Theory and Applications: Problems with Ordinary Differential Equations*. Springer, New York.

[23] Liberzon D (2012) *Calculus of Variations and Optimal Control Theory: A Concise Introduction*. Princeton University Press, Princeton.

[24] Bressan A, Piccoli B (2007) *Introduction to the Mathematical Theory of Control*. AIMS, Springfield.

[25] Clarke F (2013) *Functional Analysis, Calculus of Variations and Optimal Control*. Springer, London.

[26] Ames AD, Xu X, Grizzle JW, Tabuada P (2017) Control barrier function based quadratic programs for safety critical systems. *IEEE Trans Autom Control* 62:3861–3876. https://doi.org/10.1109/TAC.2016.2638961.

[27] Xiao W, Belta C (2019) Control barrier functions for systems with high relative degree. In: *Proceedings of the 58th IEEE Conference on Decision and Control*, Nice, pp 474–479. https://doi.org/10.1109/CDC40024.2019.9029455.

[28] Anderson BDO, Moore JB (2007) *Optimal Control: Linear Quadratic Methods*. Dover, Mineola.

[29] Khalil HK (2002) *Nonlinear Systems*, 3rd edn. Prentice Hall, Upper Saddle River.